MOLECULAR AND CELLULAR BIOLOGY, May 2006, p. 3902–3916 Vol. 26, No. 10
0270-7306/06/$08.00+0 doi:10.1128/MCB.26.10.3902–3916.2006

Persistent Transactivation by Meis1 Replaces Hox Function in Myeloid Leukemogenesis Models: Evidence for Co-Occupancy of Meis1-Pbx and Hox-Pbx Complexes on Promoters of Leukemia-Associated Genes

Gang G. Wang,[1,2]* Martina P. Pasillas,[1] and Mark P. Kamps[1]

Department of Pathology and Molecular Pathology Graduate Program, University of California at San Diego School of Medicine, 9500 Gilman Drive, La Jolla, California 92093,[1] and Biomedical Sciences Graduate Program, University of California at San Diego School of Medicine, 9500 Gilman Drive, La Jolla, California 92093[2]

Received 16 September 2005/Returned for modification 16 November 2005/Accepted 21 February 2006

Homeobox transcription factors Meis1 and Hoxa9 promote hematopoietic progenitor self-renewal and cooperate to cause acute myeloid leukemia (AML). While Hoxa9 alone blocks the differentiation of nonleukemogenic myeloid cell-committed progenitors, coexpression with *Meis1* is required for the production of AML-initiating progenitors, which also transcribe a group of hematopoietic stem cell genes, including *Cd34* and *Flt3* (defined as *Meis1*-related leukemic signature genes). Here, we use dominant *trans*-activating (Vp16 fusion) or *trans*-repressing (*engrailed* fusion) forms of Meis1 to define its biochemical functions that contribute to leukemogenesis. Surprisingly, Vp16-Meis1 (but not *engrailed*-Meis1) functioned as an autonomous oncoprotein that mimicked combined activities of Meis1 plus Hoxa9, immortalizing early progenitors, inducing low-level expression of *Meis1*-related signature genes, and causing leukemia without coexpression of exogenous or endogenous *Hox* genes. Vp16-Meis1-mediated transformation required the Meis1 function of binding to Pbx and DNA but not its C-terminal domain (CTD). The absence of endogenous *Hox* gene expression in Vp16-Meis1-immortalized progenitors allowed us to investigate how Hox alters gene expression and cell biology in early hematopoietic progenitors. Strikingly, expression of *Hoxa9* or *Hoxa7* stimulated both leukemic aggressiveness and transcription of *Meis1*-related signature genes in Vp16-Meis1 progenitors. Interestingly, while the Hoxa9 N-terminal domain (NTD) is essential for cooperative transformation with wild-type Meis1, it was dispensable in Vp16-Meis1 progenitors. The fact that a dominant transactivation domain fused to Meis1 replaces the essential functions of both the Meis1 CTD and Hoxa9 NTD suggests that Meis-Pbx and Hox-Pbx (or Hox-Pbx-Meis) complexes co-occupy cellular promoters that drive leukemogenesis and that Meis1 CTD and Hox NTD cooperate in gene activation. Chromatin immunoprecipitation confirmed co-occupancy of Hoxa9 and Meis1 on the *Flt3* promoter.

Meis1 (*m*yeloid *e*cotrophic *i*nsertion *s*ite *1*) encodes a homeodomain (HD) transcription factor that positively regulates the expansion and pool size of hematopoietic stem cells (HSCs) and is commandeered in leukemic transformation. Meis1 belongs to the three-amino-acid loop extension family of HD proteins that includes Pbx, which heterodimerizes with Meis1 (9). While *Pbx* genes are broadly expressed in hematopoiesis, *Meis1* expression is high in Sca-I$^+$ Lin$^-$ HSCs but down-regulated during transition to Lin$^+$ lineages (4, 15, 37). A positive role of Meis1 in HSC expansion is suggested in *Meis1*$^{-/-}$ mice, which exhibit severe reduction in the number and colony-forming potential of HSCs (4, 15). Hoxa9, which is also expressed specifically in progenitors and required for the expansion and repopulating abilities of HSCs (29, 37, 47), binds both Meis1 and Pbx, suggesting that combinations of Meis-Pbx, Hox-Pbx, and Hox-Pbx-Meis complexes, such as those that regulate *Hoxb1* and *Hoxb2* expression (16, 21), may also target promoters that control HSC expansion.

The functions of Meis, Pbx, and Hox proteins are usurped in leukemogenesis. Originally, *Meis1* was discovered as one of two genes activated by proviral integration in BXH2 murine acute myeloid leukemia (AML), the second being *Hoxa9* or *Hoxa7* (32, 33). Over 50% of human AML and virtually all acute lymphoblastic leukemias containing translocations of the mixed lineage leukemia (MLL) gene exhibit strong expression of MEIS1, HOXA9, and HOXA7 (2, 17, 30). In murine AML models, Meis1 dramatically accelerates leukemia initiated by Hoxa9, Hoxb6, or Hoxb3 (reduces latency from ~200 days to ~60 days) yet exhibits no independent ability to cause disease by itself (13, 28, 46). Dominant activating forms of the MEIS1-interacting protein PBX1 [E2A-PBX1, produced by the t(1;19) translocation in human pre-B leukemia (24)] and HOXA9 [NUP98-HOXA9, produced by the t(7;11) of human AML (8)] also induce AML in mouse models, suggesting that activation of the same subset of Meis1-Pbx-Hox target genes may underlie leukemic transformation.

Hox and Meis1 have distinct roles in progenitor immortalization and in regulating gene expression. Hoxa9 blocks differentiation of cultured myeloid progenitors that do not express endogenous *Meis1/2/3* and do not cause leukemia when transplanted into syngeneic recipients (7, 47, 49). Coexpression of *Meis1* plus *Hoxa9* in cultured progenitors immortalizes an earlier myeloid progenitor that induces AML in syngeneic recipients. The leukemia stem cell (LSC) phenotype induced by

* Corresponding author. Mailing address: Leichtag 249B, UCSD Medical School, 9500 Gilman Dr., La Jolla, CA 92093. Phone: (858) 534-5822. Fax: (858) 534-4715. E-mail: gawang@ucsd.edu.

Meis1 is paralleled expression of a set of leukemia-associated genes, including *Cd34*, *Flt3*, and *Erg*, which have been therefore defined as *Meis1*-related leukemic signature genes, and we hypothesized that these *Meis1* signature genes are important for LSCs to survive and expand in marrow stem cell niches (49). Whether the expression of *Meis1*-related signature genes requires Hoxa9 function is unknown, but it is now strongly implicated by our results presented below.

Equally unclear is the type of transcriptional activity that Meis1-Pbx complexes use to induce the LSC phenotype. Whereas Pbx can mediate repression through its recruitment of corepressors such as histone deacetylases and mSin3, Meis1 contains a C-terminal domain (CTD) that can promote transactivation in response to cell signals such as those induced by protein kinase A (16, 40). By interacting with both Hox and non-Hox factors (e.g., MyoD [6] and Oct1 [38]), Meis1-Pbx complexes contribute to both gene activation (e.g., of *Myogenin* [6], *Hoxb1* [16], *Hoxb2* [21], and *Pax6* [51]) and gene repression (e.g., of *CYBB* [5]). It is not clear whether activation, repression, or both functions mediate the role of Meis1 in leukemia.

Here, we ask whether activation or repression by Meis1 plays the more important role in myeloid leukemogenesis by fusing Meis1 to a dominant activation domain of Vp16 or a dominant repression domain of *engrailed*. This same strategy was used to identify transcriptional functions of the *Drosophila melanogaster Meis1* homologue, *Homothorax*, that contribute to embryonic development (18). Strikingly, in the absence of coexpressed *Hoxa9*, Vp16-Meis1 alone was able to immortalize early hematopoietic progenitors in culture that caused myeloid leukemia in syngeneic mice. Neither the immortalized progenitors nor the leukemia cells derived from them expressed endogenous *Hox* genes. The transforming ability of Vp16-Meis1 required interaction with Pbx and binding to DNA but not the function of the Meis1 CTD, which is required for cooperative leukemogenesis by wild-type Meis1 with Hoxa9. Vp16-Meis1 progenitors expressed low to moderate levels of the same *Meis1*-related leukemic signature genes (e.g., *Flt3*, *Cd34*, *Erg*, and *Msi2h*). Surprisingly, retroviral expression of *Hoxa9* or *Hoxa7* in Vp16-Meis1-expressing progenitors strongly up-regulated these *Meis1*-associated signature genes, promoted cell division, and reduced disease latency to less than 30 days. This is the first evidence that Hox proteins contribute to transcriptional activation of *Meis1*-related signature genes. Hoxa7, which also cooperates with Meis1 to induce AML, induced the same cellular and genetic changes as Hoxa9. Strikingly, the N-terminal domain (NTD) of Hoxa9 (residues 1 to 138), which is essential for its transforming properties with Meis1, was unnecessary for promoting proliferation and transcription of *Meis1* signature genes (such as *Flt3*) in Vp16-Meis1 progenitors. Taken together, these results indicate that transactivation represents the key function of Meis1 that contributes to leukemogenesis and that Meis, Hox, and Pbx proteins form a common regulatory complex that activates transcription through mechanisms dependent on the Hoxa9 NTD and the Meis1 CTD, functions that can be replaced by the Vp16 domain fused onto Meis1. Consistent with this hypothesis, chromatin immunoprecipitation (ChIP) revealed that Hoxa9 and Meis1 were both recruited to the *Flt3* promoter.

MATERIALS AND METHODS

Plasmid construction and retroviral expression system. The murine stem cell virus (MSCV) retroviral expression system for Meis1 and Nup98-Hoxa9 was described previously (8, 49). The NCBI accession numbers designating the nucleotide and protein sequences of the murine *Meis1a* isoform used are U33629 and AAA85508, respectively. Vp16-Meis1 and en-Meis1 were created by inserting sequences encoding the Vp16 activation domain or the *engrailed* repression domain into an MluI site made by mutating the first two codons of Meis1. Vp16-Meis1 mutants were generated as described elsewhere for Meis1 (49). Flag-Hoxa7 was generated by inserting the Flag tag at the N terminus of Hoxa7, and the bicistronic MSCV vector used for coexpression of Meis1 and Hoxa7 was constructed with Flag-Meis1 upstream of the internal ribosomal entry site (IRES) and Flag-Hoxa7 downstream of the IRES (49). Internal deletions in Hoxa9 were generated by excising cDNA regions flanked by two MluI sites created by site-directed mutagenesis in the MSCV-Neo vector encoding tagged Hoxa9 (7). Plasmids containing the Vp16 activation domain or *engrailed* repression domain were kindly provided by Adi Salzberg (18), and MLL-ENL was provided by Robert Slany. All constructs were verified by sequencing.

Infection and culture of hematopoietic progenitors. Protocols for retroviral infection and culture of primary hematopoietic progenitors in granulocyte-macrophage colony-stimulating factor (GM-CSF), stem cell factor (SCF), or Flt3 ligand (FL) were described previously (7, 49). Briefly, 2×10^5 to 4×10^5 of enriched Sca^+ Lin^- bone marrow progenitors from BALB/c mice were subjected to a single round of spinoculation-infection using 1 ml of retroviral supernatant (2×10^5 to 4×10^5/ml), followed by 3 days of drug resistance selection (0.6 to 1 mg/ml of G418 for MSCV-Neo or 1 μg/ml of puromycin for MSCV-Puro [drug selection is optional]), and cultured in medium containing either GM-SCF, SCF, or FL. Proliferation kinetics were evaluated by plating 2×10^5 to 4×10^5 drug-resistant Lin^- progenitors in a 12-well tissue culture plate (Corning, New York) and splitting every 3 to 4 days in fresh medium, using a protocol that keeps the progenitor number lower than 2×10^6 per well. For coexpression of Meis1 with Hoxa9 mutants, equal amounts of retrovirus encoding Flag-Meis1 (MSCV-Puro) and Hoxa9 (MSCV-Neo) were combined and used for infection, followed by dual drug selection and cultivation in SCF or FL. Wright-Giemsa staining and fluorescence-activated cell sorter (FACS) analysis were performed as described elsewhere (49).

Antibodies and immunoblotting. Ten microliters of total cellular protein (10^7 cells per ml) was used for immunoblotting. Anti-Flag, anti-Flt3, and anti-Hoxa9 were obtained and used as described previously (49). Anti-Pbx was obtained from Santa Cruz Biotechnology (C-20; sc-888).

Luciferase reporter assays. Cooperative transactivation by Vp16-Meis1 and Pbx1a was evaluated using 7xPRS-pGL3, a pGL3 luciferase derivative driven by seven tandem repeats of the *P*bx1-Meis1-*r*esponsive *s*equence (PRS), TGATT GAT, which was first identified as an E2a-PBX1 binding site (27) and later demonstrated to be recognized by Meis1 plus Pbx1 (26). One microgram of 7xPRS-pGL3 was cotransfected with 1 μg of MSCV–Vp16-Meis1, 0.5 μg of pcDNA3-Pbx1a, and 0.2 μg of pRL-TK (internal control that expresses *Renilla* luciferase persistently) into 293T cells. At 48 h after transfection, cell lysate was prepared and quantified for firefly and *Renilla* luciferase activity using a dual luciferase reporter system (Promega) and LMaxII luminometer (Molecular Devices, California). Luciferase measurements were calculated as firefly luciferase units versus *Renilla* luciferase units. Transcriptional activation was compared to basal luciferase levels in cells cotransfected with 7xPRS-pGL3, empty MSCV, and Pbx1a.

Semiquantitative RT-PCR and real-time qPCR. Total RNA was extracted (49) from immortalized progenitors 6 to 8 weeks post-retroviral infection, when normal progenitors are no longer present and when immortalized progenitors exhibit stable proliferation, stable expression of surface markers, and little to no differentiation. First-strand total cDNA, used as a template for reverse transcription-PCR (RT-PCR) and quantitative PCR (qPCR), was generated with the SuperScript reverse transcription system (Invitrogen) by using 4 μg of total RNA and 50 ng of random hexamers. Real-time qPCR was performed using 4 μl of 1:10-diluted cDNA as a template, 400 nM of primers, and SYBR Green PCR master mix (Applied Biosystems) in a 15-μl reaction volume and an Mx3000P real-time PCR system (Stratagene). The housekeeping gene *Gapdh* was used as control for mass of cDNA. The specificity and relative signal intensity of real-time qPCR amplifications were analyzed according to the manufacturer's specifications (Stratagene). Primers covered at least one intron-exon boundary. Semiquantitative RT-PCR was performed as described elsewhere (49). The sequences of primers used for each murine gene were as follows: for *Gapdh*, 5′-ATGAC ATCAAGAAGGTGGTGAAG and 5′-TCCTTGGAGGCCATGTAGG; for *Hoxa9*, 5′-TGGTTCTCCTCCAGTTGATAG and 5′-AGAAACTCCTTCTCCA

GTTCC; for *Hoxa7*, 5′-CGGGCTTATACAATGTCAACAG and 5′-AAATGG AATTCCTTCTCCAGTTC; for *Hoxa5*, 5′-GCAAGCTGCACATTAGTCAC and 5′-GCATGAGCTATTTCGATCCT; for *Hoxa10*, 5′-GGAAGGAGCGAG TCCTAGA and 5′-TTCACTTGTCTGTCCGTGAG; for *Flt3*, 5′-AAATCCCA GAAGGAGTTTGG and 5′-CGCATAGAAGGAGATGTTGTC; for *Erg*, 5′-G ACCACAAATGAGCGCAGAG and 5′-CTTTGGACTGAGGGGTGAGG; for *Cd34*, 5′-ACAGCAGTAAGACCACACCAGC and 5′-AGACACTAGCAC CAGCATCAGC; for *Il7r*, 5′-CTGACCTGAAAGTCGTTTATCGC and 5′-CA TCCTCCTTGATTCTTGGGTTC; and for *Msi2h*, 5′-ACGATTGACCCAAAA GTTGC and 5′-ACAAAGCCAAACCCTCTGTG.

In vivo leukemogenesis assay. The leukemic potential of oncogenes was evaluated in sublethally irradiated syngeneic BALB/c mice (450-rad dosage) followed by tail vein injection with 2×10^6 immortalized progenitors cultured ex vivo for 4 to 8 weeks (49) or with 5×10^5 ScaI$^+$ Lin$^-$ progenitors that were prestimulated in a cytokine cocktail containing murine SCF (1:100 dilution of culture supernatant of SCF-secreting cell lines), 10 ng/ml of murine interleukin-3 (IL-3; PeproTech Inc., New Jersey), 10 ng/ml of IL-6 (PeproTech), IL-7 (1:100 dilution of culture supernatant of IL-7-secreting cell lines), and 5 ng/ml FL (Sigma); infected with retrovirus; subjected to drug resistance selection for 2 days; and cultured for 2 more days in nonselection medium containing the same cytokine cocktail. SCF- or IL-7-containing supernatant from cytokine-secreting cell lines (SCF-secreting CHO cells and IL-7-secreting J558 cells) was harvested every 24 h as 50 ml of total medium from 15-cm plates of highly confluent cells (45). Mice exhibiting a leukemia phenotype (scruffy fur, lethargy, paralysis, or splenomegaly) were sacrificed, and cells isolated from leukemic tissues were subjected to further analysis, including flow cytometry, Wright-Giemsa staining, secondary injection, immunoblotting, retroviral integration site analysis by Southern blotting, and RT-PCR (45).

Affymetrix microarray analysis. Total RNA from 5×10^7 to 10×10^7 progenitors cultured in SCF was purified using a Maxi RNA isolation kit (QIAGEN). Gene expression profiling was examined by using the Affymetrix GeneChip Mouse Genome 430 2.0 array probed with total RNA (MicroArray Core Facility, UCSD-VA Medical Center). After normalization of overall signal intensities among different hybridization experiments, levels of gene expression were calculated using d-CHIP software, taking into consideration both the perfect match (PM) and mismatch (MM) values for all 11 sets of oligonucleotide probes representing each gene (49). At signal intensities of less than 50, the PM versus MM ratio approached unity; therefore, any signal below 50 units was designated background. Because computation analysis methods will include false positives selected due to high-level expression indicated by only one or a few of the 11 pairs of diagnostic oligonucleotides, all d-CHIP results were confirmed by visual inspection of normalized chip raw data, and a subset of genes was confirmed by semiquantitative or real-time PCR.

Two approaches were used to characterize leukemogenesis genes in Vp16-Meis1 progenitors: (i) identification of genes up-regulated threefold or greater in Vp16-Meis1 progenitors by comparison to nonleukemic Hoxa9 progenitors, and (ii) identification of genes up-regulated threefold or greater by Hoxa9 in Vp16-Meis1 progenitors. Among 39,000 genes represented on the array, only 24 genes were up-regulated >3-fold in three of the Vp16-Meis1 progenitor lines by comparison to five of the Hoxa9 progenitor lines, and only 77 genes (which included 22 of those 24 genes induced by Vp16-Meis1) were up-regulated >3-fold by expression of Hoxa9 in each of the Vp16-Meis1 progenitor lines, demonstrating that in both cases, the transcriptional impact of the oncoprotein is specific and limited. Among those 24 genes induced by Vp16-Meis1 were 16 of the original 25 genes we reported as *Meis1*-related signature genes that were expressed specifically in leukemogenic Hoxa9-plus-Meis1 progenitors but not in Hoxa9 progenitors (i.e., *Cd34*, *Flt3*, *Il7r*, *Crlr*, *Erg*, *Gpr56*, *Tilz1b*, *Nrip1*/*RIP140*, *C1qr1*, *Tmsb10*, *Kcna3*, *Ngn*, *Ptprcap*/*CD45AP*, *Satb1*, *Ngn*, and *Ly86*/*MD-1*) (see Table 3, below). The other nine of the original *Meis1* signature genes, expressed at extremely low levels in our original analysis of Hoxa9-plus-Meis1 progenitors, have been eliminated as candidate leukemogenesis genes based on their inconsistent activation in additional cell lines immortalized by Hoxa9 plus Meis1, lack of their expression in Vp16-Meis1 progenitors, and lack of activation by Hoxa9 (*Tspan2*, *CD244*, *Gem*, *PLZF*, *Cd27*, *Itgb7*, *Oaf*, *CXXC5*, and *Ebf*). The eight new genes activated by Vp16Meis1 (*Msi2h*, *Sox4*, *Dbx4*, *P2x*, *Bcl2*, and *Sesn3*, plus two unknown expressed sequence tags) were also expressed at significantly higher levels in Hoxa9-plus-Meis1 progenitors than in Hoxa9 progenitors and were added to the genes shown below in Table 3. The remaining 54 genes that were activated by Hoxa9 in Vp16-Meis1 progenitors (except c-*kit*, listed below in Table 3) were not expressed in Hoxa9 progenitors or Hoxa9-plus-Meis1 progenitors; therefore, they may be artificial targets of Hoxa9 in the context of Vp16-fused Meis1 or they may be real targets under different cellular contexts that were mimicked/activated by Vp16-Meis1. However, their activation is physiologically irrelevant to leukemogenesis by Hoxa9 plus Meis1 (they are not included in Table 3; information is available upon request).

Retrovirus integration site analysis. Genomic DNA was purified, digested, resolved, and transferred to a membrane as previously described (49). EcoRI or BamHI was used to digest DNA from progenitors infected by retrovirus encoding Vp16-Meis1 or Meis1-IRES-Hoxa7, respectively, and cDNA fragments encoding the Vp16 activation domain and Hoxa7 were used for making probes.

EMSA. Heterodimerization of Hoxa9 with either Pbx1 or Meis1 on DNA was examined by electrophoretic mobility shift assay (EMSA), as described previously (7, 43).

ChIP analysis. ChIP analysis was performed according to a modified protocol based on ChIP protocols of Upstate Biotechnology (New York) and Active Motif (California). Briefly, 2×10^7 to 3×10^7 myeloid progenitors were collected and subjected to DNA-protein cross-linking in 10 ml of phosphate-buffered saline plus 1% formaldehyde for 10 to 15 min at room temperature, followed by a 5-minute treatment in 5 ml of 0.125 M glycine (supplemented with 1× Complete protease inhibitor cocktail [PIC; Roche]) to stop the cross-linking reaction. After washing with cold phosphate-buffered saline–1× PIC, the cell pellet was suspended in 200 μl of sodium dodecyl sulfate lysis buffer (Upstate; 1× PIC added), incubated on ice for 15 min, and then subjected to three repeats of 12- to 13-second sonication (Sonifier 450 [VMR Scientific]). Sheared DNA was 400 bp to 1.5 kbp. The sheared sample was centrifuged at 14,000 rpm for 15 min at 4°C, and the supernatant was diluted 1:10 with ChIP dilution buffer (Upstate; 1× PIC added). The chromatin was immuno-precleared with 60 μl salmon sperm DNA-protein A-agarose (Upstate) per 2 ml chromatin, followed by a 1-h rotation (4°C) and removal of the agarose by 2 min of centrifugation at 1,500 rpm. Five hundred microliters of chromatin was used for overnight immunoprecipitation by control antibody (immunoglobulin G [IgG]) or specific antibody with rotation at 4°C. Sixty microliters of protein A-agarose was added to each tube followed by rotation for 2 h and sequential washing with low-salt wash buffer, high-salt wash buffer, LiCl wash buffer, and Tris-EDTA buffer as described elsewhere (Upstate; 1× PIC added to all buffers). Chromatin was eluted twice with 100 μl of freshly made 1% sodium dodecyl sulfate plus 0.1 M $NaHCO_3$ with 15 min of vigorous shaking on a vortex mixer. A 200-μl aliquot of eluted chromatin-protein was subjected to reverse cross-linking, removal of RNA (by addition of 8 μl of 5 M NaCl and 1 μl of RNase A [10 μg/μl] and incubation at 65°C for 6 to 16 h), and then removal of protein (by subsequent addition of 4 μl of 0.5 M EDTA, 8 μl of 1 M Tris-HCl [pH 6.5], and 1 μl of 20-mg/ml protease K, with incubation at 45°C for 1 to 2 h). DNA was recovered using a QIAQuick spin column and suspended in 100 μl of elution buffer (QIAGEN). PCR amplification was performed using 1 U of Platinum *Taq* polymerase (Invitrogen) and 2 to 4 μl of eluted DNA.

Antibodies for ChIP (amount added per 500 μl of chromatin) included M2 anti-Flag (8 μg; Sigma), anti-Hoxa9 HD (10 μg), anti-Meis1 HD (10 μg), anti-Meis1 N terminal (10 μg; gift of Mark Featherstone), anti-acetyl-histone H3 (1 μg; Upstate 06-599) and anti-dimethylated histone H3 Lys4 (anti-H3K4Me2 [1 μg]; Upstate 07-030).

The murine *Flt3* genomic structure was deduced using information provided by the UCSC Genome Browser (http://genome.ucsc.edu), and the putative transcription start site was defined using in silico mapping of common 5′ expressed sequence tag sequences onto the genomic sequence. The ChIP primers used to amplify regions of the *Flt3* locus were P3 (5′-GGACAAATGGCTCAGGAGGG and 5′-CATCTGGTAGATCTGCATTGTGG), P4 (5′-CTAGATGTGGCTCT GGGAACC and 5′-AGACAGATAGACAGAGTGCCAGC), P5 (5′-AGTCA GAAGGGACTGGCTCC and 5′-GAGTGCTGCTTAGCAGATTACC), and P6 (5′-CCTCAGAAGTGAACTCAGTTTCC and 5′-CTGCATCCAGACCAT GAAGG).

RESULTS

Hoxa7 mimics Hoxa9 in its independent and Meis1-dependent leukemic properties. *Hoxa7* is also coactivated with *Meis1* in BXH-2 murine AML (32); however, its leukemic functions have not been described in experimental models. Therefore, *Hoxa7* was cloned into the MSCV retroviral vector, and its independent and Meis1-dependent transforming functions were assessed. Like Hoxa9, Hoxa7 immortalized GM-CSF-dependent (Fig. 1A and E) or SCF-dependent (Fig. 1B) progenitors in the absence of coexpressed *Meis1*. Like Hoxa9-immortalized progenitors, Hoxa7-immortalized progenitors were 100% MacI$^+$ (data not shown), differentiated into mature

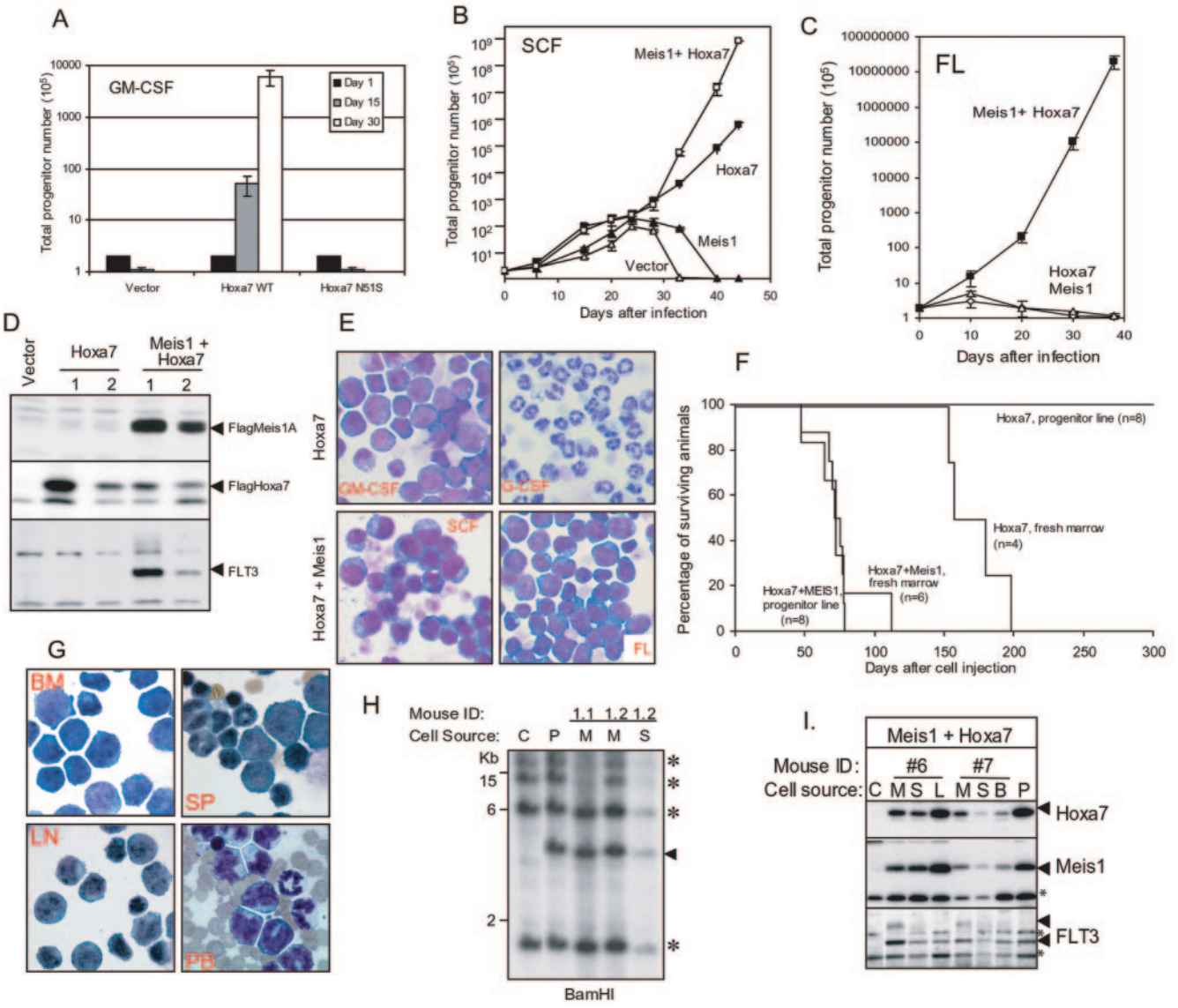

FIG. 1. Hoxa7 mimics Hoxa9 in terms of its independent and Meis1-dependent transforming functions. (A) Growth kinetics of GM-CSF-dependent marrow progenitors infected with MSCV retrovirus encoding vector only, wild-type (WT) *Hoxa7*, or a DNA-binding-defective *Hoxa7* (N51S), followed by drug selection. Error bars indicate the standard deviations among three repeated experiments. (B and C) Growth kinetics of primary marrow progenitors infected with retrovirus encoding vector only, *Meis1*, *Hoxa7*, or *Meis1* plus *Hoxa7*, followed by culture in SCF (B) or in FL (C). (D) Immunoblot analysis of Hoxa7, Meis1, and Flt3 in cultures shown in panel B. (E) Wright-Giemsa stain of GM-CSF-dependent progenitors immortalized by Hoxa7 in GM-CSF or when shifted to G-CSF and those immortalized by Meis1 plus Hoxa7 in SCF or FL. (F) Survival curves of mice injected with two progenitor lines immortalized by *Hoxa7* in SCF (four for each), progenitors immortalized by coexpressed *Meis1* and *Hoxa7* (four for one line in SCF and four for one line in FL), and Sca^+ Lin^- marrow progenitors freshly transduced with retrovirus encoding *Hoxa7* (four mice) or *Meis1* plus *Hoxa7* (six mice). (G) Representative Wright-Giemsa stains of tissue samples from mice bearing AML induced by Meis1 plus Hoxa7. BM, bone marrow; SP, spleen; LN, lymph node; PB, peripheral blood. (H) Southern blot of retroviral integration sites, using BamHI-digested genomic DNA from control Hoxa9-immortalized progenitors (C), injected parental progenitors immortalized by Meis1 plus Hoxa7 (P), and leukemic cells extracted from bone marrow (M) or spleen (S). The arrowhead indicates a band that represents the proviral Hoxa7 integration site. Stars indicate nonspecific bands. ID, identification. (I) Immunoblot analysis of expression of retrovirus-encoded genes, Flag-tagged Hoxa7 and Meis1, and Flt3 in control Hoxa9-immortalized progenitors (C); in parental progenitors immortalized by Meis1 plus Hoxa7 that were injected into mice (P); in leukemia cells from bone marrow (M), spleen (S), and lymph node (L); and in purified white blood cells (B). The arrowhead indicates a specific band, and the star indicates a nonspecific band.

neutrophils when shifted into medium containing G-CSF (Fig. 1E), and did not cause leukemia when injected into sublethally irradiated mice (Fig. 1F). Similar to the effect of coexpressing *Meis1* with *Hoxa9*, coexpression of *Meis1* with *Hoxa7* immortalized a distinct SCF-dependent progenitor (Fig. 1B and E) that expressed Flt3 (Fig. 1C and D), proliferated more rapidly (Fig. 1B), underwent self-renewal in FL (Fig. 1C and E) or IL-7, GM-CSF, or SCF plus G-CSF (data not shown), and induced myeloblastic leukemia (Fig. 1F and G) (Mac-I^+ $B220^-$ $Cd19^-$) that exhibited the same pathophysiology as that

TABLE 1. Phenotypes of leukemias induced by coexpressed *Hoxa7* and *Meis1*[c]

Cell type injected	Latency (days)	Organ wt (mg)		WBC count (1,000/μl)[b]	Leukemia FACS[a]	
		Spleen	Node		$MacI^+$	$B220^+$
Hoxa7 + *Meis1* (progenitor line)	70 ± 10	500 ± 100	26 ± 5	85 ± 17	78 ± 16	25 ± 6
Hoxa7 + *Meis1* (fresh marrow)	74 ± 21	637 ± 200	31 ± 6	92 ± 12	80 ± 18	18 ± 9

[a] FACS results (percentage) of leukemia cells from spleen and bone marrow.
[b] WBC, white blood cells in peripheral blood.
[c] Values are averages ± standard deviations.

induced by *Hoxa9* plus *Meis1* (Table 1). Leukemic cells contained the same retroviral integration sites as injected progenitors (Fig. 1H) and expressed retroviral Flag-Hoxa7 and Flag-Meis1 and endogenous Flt3 (Fig. 1I), confirming that they arose from injected cells.

In contrast to the use of stably immortalized progenitors to initiate leukemia, we also reconstituted mice with Sca^+ Lin^--enriched marrow progenitors following an immediate infection with *Hoxa7* or *Hoxa7* plus *Meis1* retrovirus. Mice transduced with *Hoxa7*-infected progenitors developed myeloid leukemia after a long latency (170 days), while those transduced with *Hoxa7* plus *Meis1* acquired AML rapidly (74 days) (Fig. 1F) with leukemic myeloblasts that evidenced the same phenotypes as those resulting from injections of immortalized progenitor lines (Table 1). Therefore, Hoxa7 behaved the same as Hoxa9, as both immortalized a nonleukemic myeloid progenitor when expressed without *Meis1* and immortalized an $Flt3^+$, leukemia-initiating progenitor when coexpressed with *Meis1* (49).

Vp16-Meis1 immortalizes hematopoietic progenitors in the absence of coexpressed *Hox* genes. To identify the transcriptional function of Meis1 that is important for cooperation with Hoxa9 and Hoxa7 in establishing the leukemic stem cell phenotype, dominant transactivating or transrepressing forms of Meis1 were produced by fusing it to the activation domain of herpes simplex viral protein Vp16 or to the repression domain of *Drosophila engrailed* (en) (Fig. 2A). $Sca1^+$ Lin^--enriched marrow progenitors were infected with retrovirus encoding empty vector, Meis1, Vp16-Meis1, or en-Meis1 and cultured in medium containing SCF or FL as the sole cytokine. With either cytokine, expression of Vp16-Meis1 itself was able to immortalize progenitors, while cultures infected with Meis1 or en-Meis1 retrovirus followed the same decline in progenitors as uninfected cultures (Fig. 2B). Vp16-Meis1 had no effect on NIH 3T3 fibroblasts, indicating that the differentiation arrest phenotype was not accompanied by a cell proliferation phenotype, as is the case with E2A-PBX1, a transcriptionally activated form of the MEIS1 partner PBX1 (25). To test whether immortalization by Vp16-Meis1 might be mediated by expression of endogenous *Hox* genes, the expression of *Hoxa5*, *Hoxa7*, *Hoxa9*, and *Hoxa10* was measured by semiquantitative RT-PCR (Fig. 2C) and quantitative real-time PCR (data not shown, except for Hoxa9 in Fig. 4D, below). None of these four *Hox* genes was expressed in two of the Vp16-Meis1-immortalized progenitors, while they were all expressed strongly in progenitors immortalized by the *Hox* locus transactivators MLL-ENL (50) or Nup98-Hoxa9 (8). A global view of *Hox* gene expression assessed by using Affymetrix mouse gene arrays demonstrated no expression of any of 31 *Hox* genes present on the array chip (*Hoxa1* to *-5*, *-a7*, *-a10*, *-a11*, *-a13*, *-b1*, *-b3* to *-9*, *-b13*, *-c4* to *-6*, *-c8*, *-c9*, *-c13*, *-d1*, *-d3*, *-d4*, or *-d10* to *-13*) among five independent Vp16-Meis1 progenitor lines (19), while each of two Nup98-Hoxa9-immortalized progenitor lines exhibited strong expression of eight *Hox* genes (*Hoxa5*, *-a7*, *-a9*, *-a10*, *-c4* to *-6*, and *-c8*). Therefore, *Hox* genes are not expressed in Vp16-Meis1 progenitors. Affymetrix arrays also revealed strong expression of Pbx1a, weak expression of Pbx2a, and no expression of Pbx1b, Pbx2b, or Pbx3 in Vp16-Meis1 progenitors (Fig. 2E). Pbx1a expression was verified by Western blotting (Fig. 2D). Vp16-Meis1 progenitors were cytokine dependent, proliferating as progenitors in SCF or FL, and a subset (5 to 25%) proliferated as undifferentiated progenitors in IL-7, GM-CSF, or G-CSF (Fig. 2F and G), a behavior similar to progenitors coexpressing *Hoxa9* plus *Meis1* (49). Thus, Vp16-Meis1 mimics the combined activities of Hoxa9 plus Meis1, immortalizing progenitors capable of responding to both lymphoid and myeloid cytokines. The ability of a dominant activating form of Meis1 to replace the immortalizing function of Hox proteins raises the possibility that Meis1 binds the same promoters as Hoxa9 and Hoxa7 and that the histone acetyltransferase (HAT) activity recruited by Vp16 (31) replaces an intrinsic Hox-dependent activation function.

Vp16-Meis1-mediated immortalization requires binding to Pbx and to DNA but not the function of the Meis1 CTD, an essential domain for cooperation of wild-type Meis1 with Hoxa9. The immortalization potential of Vp16-Meis1 corresponded to its ability to induce cooperative transactivation with Pbx1. A mutation that eliminated the entire M1-M2 Pbx interaction domain (Δ64-202), a five-residue neutral mutation in the M2 domain ($M2^{\Delta LRF/LELL}$) that disrupts heterodimerization with Pbx1 (49), or an HD mutation ($HD^{N51S/\Delta RRR}$) that virtually eliminates binding of Meis1-Pbx1 heterodimers to DNA (Fig. 3A) each reduced activation of a reporter construct driven by Pbx1-Meis1 binding motifs to levels 20% or less of those induced by wild-type Vp16-Meis1 (Fig. 3C), and each of these mutants was incapable of immortalizing progenitors in either SCF or FL (Fig. 3B). By contrast, an N-terminal deletion preceding the Pbx interaction domain (Δ1-64), a three-residue neutral mutation in M2 ($M2^{\Delta LELL}$), and an internal deletion between the M2 domain and HD (Δ202-260), all of which retained active Pbx-Meis1 heterodimerization potential on DNA (49), maintained more robust activation of the reporter construct and immortalized FL-responsive progenitors actively (Fig. 3B and C). The Meis1 CTD, which is essential for the ability of wild-type Meis1 to immortalize $Flt3^+$ progenitors in cooperation with Hoxa9, was dispensable for transactivation by Vp16-Meis1 and was also unnecessary for Vp16-Meis1-mediated immortalization of $Flt3^+$ progenitors. Immunoblot analysis confirmed expression of all

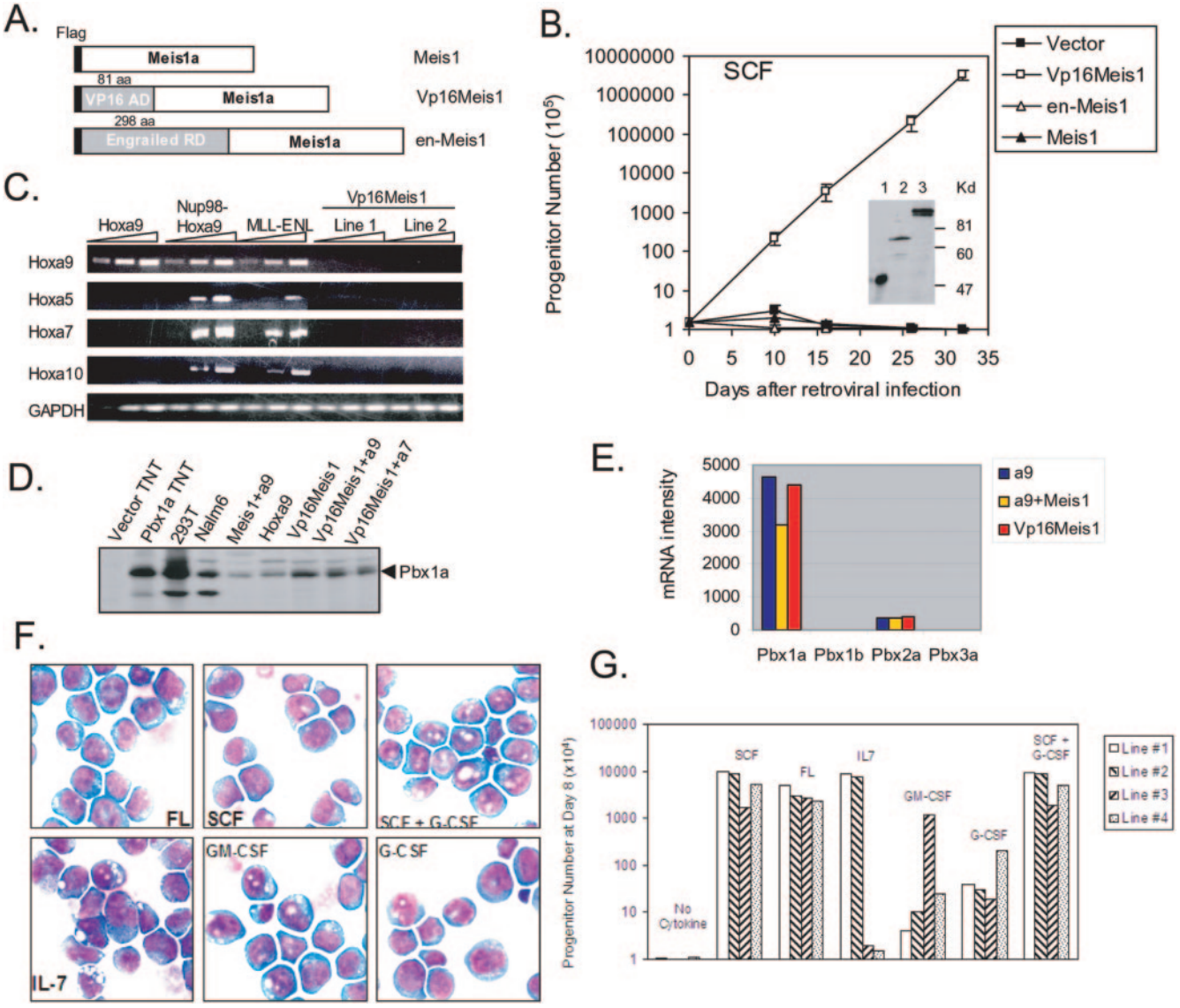

FIG. 2. Vp16-Meis1 immortalizes early hematopoietic progenitors in the absence of coexpressed *Hox* genes. (A) Depiction of Flag-tagged Meis1, Vp16-Meis1, and en-Meis1. (B) Proliferation kinetics of progenitors cultured in SCF, after infection with retrovirus encoding Vp16-Meis1, Meis1, or en-Meis1 followed by 3-day puromycin resistance selection. A total of 200,000 puromycin-resistant progenitors were plated at day 0, and culture medium was changed every 3 days. Error bars indicate standard deviations from three repeat experiments. The inserted panel indicates Western blot analysis of Meis1 (lane 1), Vp16-Meis1 (lane 2), and en-Meis1 (lane 3) expressed in NIH 3T3 fibroblasts with anti-Flag antibody. (C) Semiquantitative RT-PCR demonstrating that Vp16-Meis1 progenitors do not express *Hoxa5*, *Hoxa7*, *Hoxa9*, or *Hoxa10*, while progenitors immortalized by Nup98-Hoxa9 or MLL-ENL express these *Hox* genes. RNA was prepared from immortalized progenitor cultures 5 to 7 weeks after retroviral infection, when progenitor phenotypes were stabilized. *Gapdh* served as the cDNA internal control. Triangles indicate a 1:10 serial dilution of cDNA template from right to left. (D) Western blot analysis of Pbx1a protein levels in progenitors immortalized by Hoxa9 alone or with coexpressed Meis1 and by Vp16-Meis1 in the absence or presence of coexpressed Hoxa9/a7; positive and negative controls were 1 μl of in vitro transcription-translation (TNT) reaction mixture added with Pbx1a or empty expression vector. (E) mRNA expression level of Pbx isoforms quantified by Affymetrix arrays in progenitors immortalized by Hoxa9, Hoxa9 plus Meis1, or Vp16-Meis1. (F and G) Vp16-Meis1 progenitors proliferate in SCF or FL as the sole supporting cytokine. All four tested lines proliferated well in SCF or FL, two lines proliferated well in IL-7, and 5 to 20% of each cell line proliferated slowly in G-CSF or GM-CSF. The morphology of immortalized progenitors following Wright-Giemsa stain is illustrated in panel F, and their relative expansion in various cytokines is quantified in panel G.

retrovirus-encoded Vp16-Meis1 proteins in infected progenitors subjected to drug selection (Fig. 3D). The fact that the Vp16 transactivation domain can replace the function of the Meis1 CTD in immortalization of FL-responsive progenitors (16) supports the notion that gene activation is the essential biochemical function performed by the Meis1 CTD in establishing leukemia with Hoxa9.

Vp16-Meis1 induces basal transcription of *Meis1*-related signature genes. Previously, we demonstrated that the AML-initiating progenitors produced by coexpressed *Meis1* plus

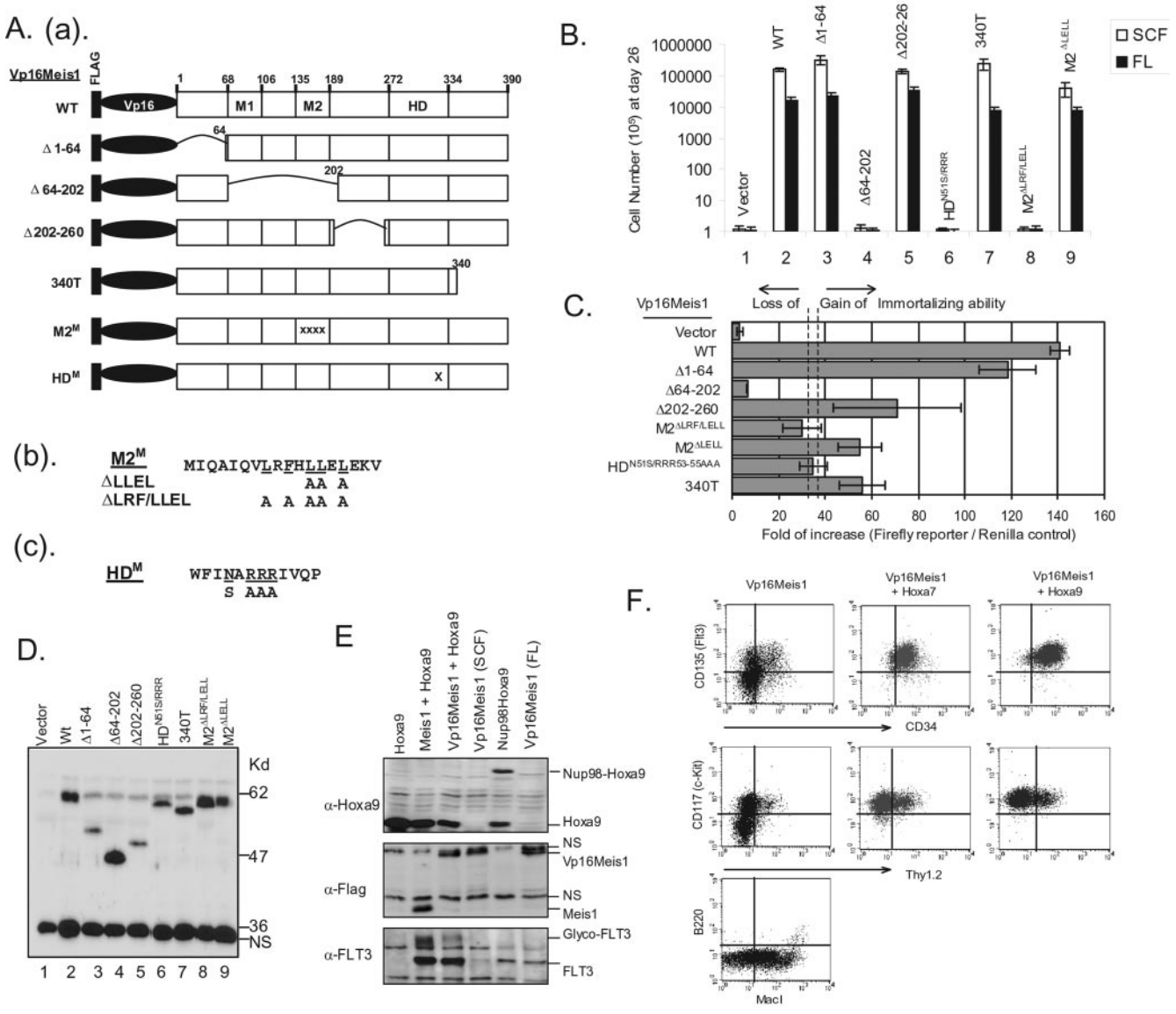

FIG. 3. Vp16 replaces the essential function of the Meis1 CTD and circumvents Hox cofactor dependence. (A) Depiction of Vp16-Meis1 wild-type and mutant constructs (a) and point mutations in M2 or in the HD (b and c). (B) Mutational analysis of domains required for immortalization by Vp16-Meis1 in SCF or FL. Plotted are the cumulative progenitor numbers after 26 days of culture following plating of 200,000 retrovirus-infected and puromycin-resistant Lin$^-$ progenitors. Error bars indicate standard deviations from three duplicate cultures. (C) Transactivation of a Pbx-Meis-responsive luciferase reporter (7xPRS-luc) by Vp16-Meis1 wild type and mutants in the presence of Pbx1a in 293T cells: increase of normalized luciferase activity. Error bars represent the standard deviations from two duplicate experiments. (D) Immunoblot using anti-Flag antibody to examine retroviral expression of Vp16-Meis1, 1 week after infection of Lin$^-$ progenitors followed by drug resistance selection shown in panel B (SCF). NS, nonspecific band. (E) Immunoblot demonstrating that Vp16-Meis1 activates a low level of *Flt3* expression in the absence of Hoxa9 (lanes 4 and 6), which is augmented by subsequent coexpression of *Hoxa9* (lane 3). (F) Typical presentation of FACS analysis of Vp16-Meis1-immortalized progenitors without (left panels) and with sequential retroviral infection of Hoxa7 or Hoxa9 (middle and right panels). Vp16-Meis1-immortalized progenitors (6 weeks after initial Vp16-Meis1 infection) were used for a sequential Hox infection, and cells were subjected to FACS analysis after cultivation for another 4 weeks.

Hoxa9 exhibited a genetic signature that includes stem cell-specific genes (i.e., *Meis1*-related signature genes, such as *Cd34*, *Flt3*, *Erg*, *Msi2h*, etc.) which were not expressed in non-leukemic progenitors immortalized by Hoxa9 alone (49). Because Vp16-Meis1 progenitors expressed *Flt3*, we evaluated the expression of other *Meis1*-related signature genes using FACS, immunoblotting, and microarray analysis. FACS demonstrated that Vp16-Meis1-immortalized progenitors were Cd34^{low} Flt3^{low} c-Kit$^{low/medium}$ MacI^{variable} B220$^-$ Cd19$^-$ Cd27$^-$ Thy1.2$^{-/low}$ (Fig. 3F), a profile similar to that of progenitors immortalized by Meis1 plus Hoxa9 (49), with the major difference being a lower level of *Cd34* and *Flt3*. Immunoblot analysis confirmed a low level of Flt3 protein in Vp16-Meis1 progenitors (Fig. 3E). Analysis of Affymetrix gene expression arrays revealed that many of the previously identified *Meis1* signature genes were expressed at low to moderate levels

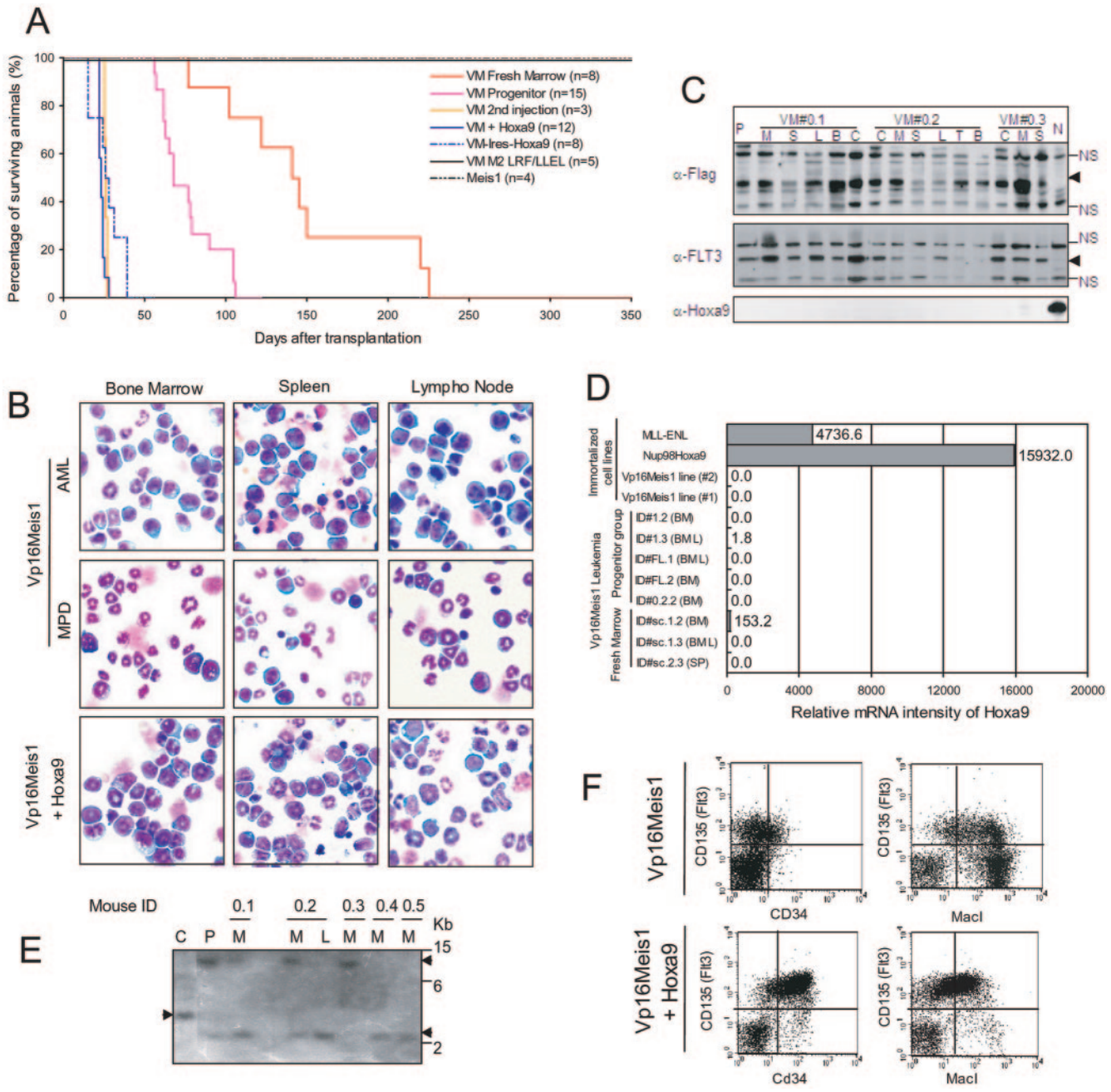

FIG. 4. Vp16-Meis1 causes AML and MPD by a mechanism independent of Hoxa7 or Hoxa9. (A) Survival curves for mice injected with Lin$^-$ marrow progenitors 48 h following infection with retrovirus expressing Vp16-Meis1 (VM, fresh marrow), a VM mutant defective in binding Pbx (M2 LRF/LELL), or Meis1, mice injected with progenitor cell lines immortalized by VM (VM progenitor) or by VM plus Hoxa9 (VM-Ires-Hoxa9), or mice injected with VM progenitors expressing retroviral Hoxa9 (VM+Hoxa9). The second injection was performed using bone marrow cells freshly extracted from a VM leukemic mouse. The *n* value indicates the cohort size (injected mice). (B) Wright-Giemsa stains of cells extracted from tissues of mice with AML or MPD induced by Vp16-Meis1 or by Vp16-Meis1 plus Hoxa9. (C) Western blot analysis of Vp16-Meis1, Flt3, and Hox in tissues from mice with leukemia caused by Vp16-Meis1. Arrowheads indicate specific bands. NS, nonspecific bands; N, Hoxa9 progenitors as a control; P, injected parental VM progenitors; M, marrow; S, spleen; L, lymph nodes; B, peripheral blood white cells; T, thymus; C, cell lines derived from marrow leukemic progenitors. (D) Real-time qPCR analysis of Hoxa9 mRNA levels in immortalized cell lines and in leukemias induced by Vp16-Meis1. Cell lines were the same as those used in Fig. 2C. Samples of leukemia induced by Vp16-Meis1 were derived from the experiment shown in panel A from either the fresh marrow group or the progenitor group. The amplicon of Hoxa9 targets sequences encoding the N-terminal domain, which does not exist in Nup98-Hoxa9. Values to the right of the bars represent relative values of Hoxa9 transcript intensity, after verification of PCR specificity, threshold setup, relative transcript intensity calculated from the cycle threshold value, and normalization against *Gapdh*. BM, bone marrow; SP, spleen; BML, leukemic cell lines from bone marrow. (E) Southern blot analysis of Vp16-Meis1-retrovirus integration sites among leukemia tissues, as indicated by arrowheads. C, a different VM progenitor line as a negative control; P, injected parental progenitors; M, bone marrow; L, lymph node. (F) FACS analysis of leukemia induced by Vp16-Meis1 alone or with coexpressed Hoxa9.

TABLE 2. Phenotypic characterization of Vp16-Meis1-induced leukemia in mice[a]

Parameter	Vp16-Meis1		Vp16-Meis1 + Hoxa9	Control (avg)
	Fresh marrow	Progenitor line		
No. of mice examined	7	11	5	4
Disease latency (days)	134 ± 49	74 ± 18	24 ± 5	NA
Organ wt (mg)				
Spleen	625 ± 213	723 ± 338	396 ± 219	106
Lymph node	58 ± 28	51 ± 39	15 ± 8	<1
Thymus	40 ± 18	51 ± 29	54 ± 27	29
Peripheral blood cell analysis				
WBC[b] (10^3/ml)	100 ± 36	58 ± 47	ND	3
Granulocytes (%)	74 ± 6	68 ± 30	ND	25
Lymphocytes (%)	23 ± 9	31 ± 27	ND	67
Platelets (10^3/ml)	370 ± 136	216 ± 105	ND	817
Hematocrit (%)	34 ± 7	40 ± 10	ND	45
FACS analysis of marrow leukemia cells (%)				
Mac-I	73 ± 15	84 ± 14	56 ± 33	NA
B220	2 ± 1	0 ± 0	10 ± 9	NA
Thy1.2	2 ± 1	1 ± 1	15 ± 10	NA
Cd135 (Flt3)	56 ± 31	28 ± 23	55 ± 33	NA
Scored as AML[c]	4	6	5	NA
Scored as MPD[c]	3	5	0	NA

[a] Values are averages ± standard derivations unless otherwise indicated. ND, not determined; NA, not applicable.
[b] WBC, white blood cells.
[c] According to the French-American-British classification, in which counts of immature myeloblasts in marrow are ≥30% for AML and ≤30% for MPD.

(see Fig. 5D and E and Table 3, below). The additional genes (identified as described in Materials and Methods), *Msi2h*, *Sox4*, *Dbx4*, *P2rx3*, *Bcl2*, and *Sesn3*, which were expressed in Vp16-Meis1 progenitors, were also found expressed at significantly higher levels in Hoxa9-plus-Meis1 progenitors than in Hoxa9 progenitors and have been added to the list of *Meis1*-related signature genes (see Table 3, below). The expression of *Cd34*, *Flt3*, *Erg*, *Msi2h*, *Il7r*, *Grp56*, and *Tizl1b* was further confirmed by semiquantitative RT-PCR (data not shown) and real-time PCR (see Fig. 5E).

Vp16-Meis1 induces AML and MPD in vivo. Activation of *Meis1*-related signature genes suggested that Vp16-Meis1 progenitors would initiate leukemia. Indeed, AML arose in each of 12 mice injected with three different Vp16-Meis1-immortalized progenitor lines (2×10^6 cells per mouse), as well as in each of 8 mice injected with Lin^- marrow progenitors freshly infected with Vp16-Meis1 retrovirus (5×10^5 cells per mouse) with a latency of 74 and 134 days, respectively (Fig. 4A and Table 2). Mice injected with progenitors transduced with a Pbx interaction-defective mutant, $M2^{\Delta LRF/LELL}$, did not develop leukemia over 370 days. Leukemia cells were factor dependent, expressed retroviral Vp16-Meis1 (Fig. 4C), and contained the same retroviral integration sites as those within the oligoclonal parental progenitors (Fig. 4E), indicating that they arose from injected cells. FACS analysis demonstrated that the majority of leukemic cells were myeloid ($Mac\text{-}I^+$ $B220^-$ $Cd19^-$ $Thy1.2^-$ $c\text{-}Kit^+$) (Fig. 4F and Table 2). Mice exhibited two forms of disease. The first (10 of 18 examined animals) was AML, in which 30 to 95% of leukemic cells stained as immature myeloblasts. The second (in 8 out of 18) was a myeloproliferative disease (MPD) in which 70 to 90% of leukemia cells exhibited significant neutrophil maturation (Table 2 and Fig. 4B). In both diseases, mice presented with 3- to 12-fold enlarged spleens, 10- to 50-fold enlarged lymph nodes, and 4- to 40-fold increases in circulating myeloid cells (Table 2). Comparable amounts of Vp16-Meis1 protein were present in myeloid cells from both diseases (data not shown), discounting the possibility of a reactive granulocytosis. Over 50% of leukemic progenitors expressed *Flt3* (FACS in Fig. 4F and Table 2 and immunoblot in Fig. 4C). Thus, Vp16-Meis1 causes myeloid leukemia with 100% penetrance, and leukemic myeloblasts retain a low level of *Flt3* and *Cd34* expression, similar to the parental cells.

Secondary recipients of leukemic marrow acquired leukemia with a much shorter latency, averaging 26 days (Fig. 4A), indicating that additional genetic change accelerates leukemogenesis initiated by Vp16-Meis1. Because *Hoxa9* and *Hoxa7* are coactivated with *Meis1* in BXH2 mouse AML, we evaluated whether *Hoxa9* or *Hoxa7* might be activated as a cooperating event during progression of Vp16-Meis-induced leukemia. Immunoblot analysis using a polyclonal antibody against the homeodomain of Hoxa9, which also detects Hoxa7 less efficiently, revealed no apparent up-regulation of these two proteins in 10 independent leukemias, regardless of whether AML arose from progenitor lines or from freshly infected marrow (Fig. 4C). This result was confirmed by real-time qPCR (Fig. 4D): in seven of eight leukemias examined (three from the fresh marrow group and the other five leukemias from the progenitor group [as in Fig. 4A]), *Hoxa5*, *Hoxa7*, *Hoxa9*, and *Hoxa10* transcripts were absent or were present at levels lower than 0.01% of that expressed in progenitors immortalized by Nup98-Hoxa9 or MLL-ENL (results for Hoxa9 are exemplified in Fig. 4D). A single exception, exhibiting a very low level of *Hoxa9* (~3% of the Hoxa9 level expressed in MLL-ENL progenitors) (sample sc1.2), also expressed *Hoxa5*, *Hoxa7*, and *Hoxa10* at levels 1 to 5% of that expressed in progenitors immortalized by MLL-ENL. Thus, the large majority of myeloid leukemias induced by Vp16-Meis1 did not acquire activation of endogenous *Hoxa7* or *Hoxa9* genes as secondary cooperating events.

Expression of *Hoxa9* or *Hoxa7* in Vp16-Meis1 progenitors induces further activation of *Meis1* signature genes, stimulates proliferation, and accelerates disease progression to the level of bona fide AML myeloblasts. An important unresolved question concerning the mechanism of cooperativity by *Hox* plus *Meis1* is whether Hoxa7 or Hoxa9 assists Meis1 in the activation of *Meis1*-related signature genes or Meis1 functions independent of coexpressed Hox proteins. Because Vp16-Meis1 progenitors expressed low levels of *Meis1*-related signature genes and expressed no endogenous *Hox* genes, they represented a good cell model to test whether Hoxa9 or Hoxa7 could further activate expression of *Meis1*-related signature genes. Strikingly, retroviral expression of *Hoxa9* or *Hoxa7* in Vp16-Meis1 progenitors induced strong proliferation (Fig. 5B), strong up-regulation of Flt3 and Cd34 proteins (Fig. 3F and 5A), and 3- to 20-fold activation of other *Meis1* signature genes (Table 3 and Fig. 5D). The reliability of the Affymetrix array analysis was verified using semiquantitative RT-PCR (data not shown) and real-time qPCR (Fig. 5E). Six newly

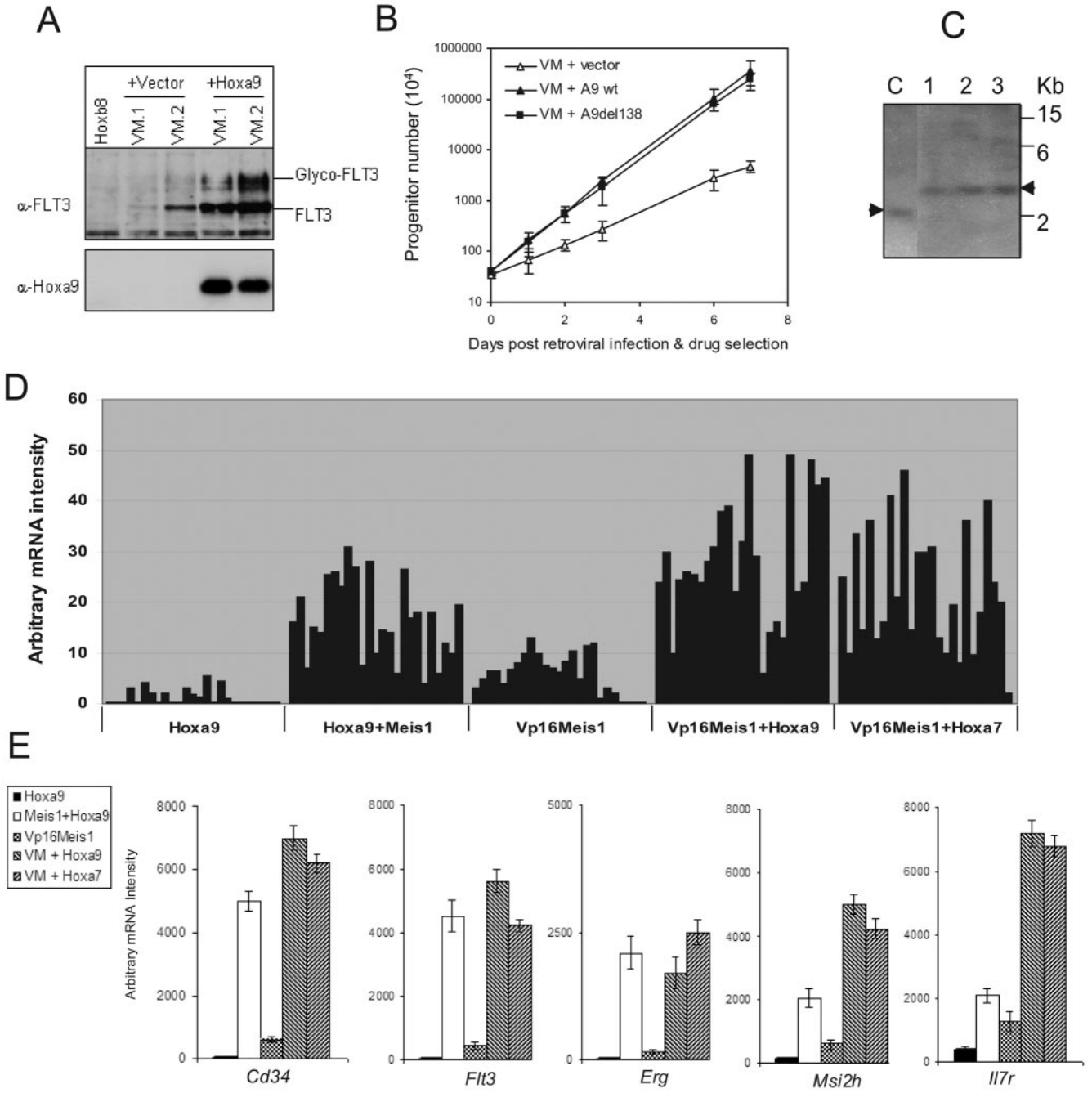

FIG. 5. Both Hoxa9 and Hoxa7 activate expression of *Meis1*-related signature genes in Vp16-Meis1 progenitors. (A) Immunoblot analysis of Flt3 in two Vp16-Meis1 progenitor lines (VM.1 and VM.2) before and after coexpression of *Hoxa9*, analyzed subsequently by Affymetrix gene arrays. (B) Proliferation rates of Vp16-Meis1 progenitors after infection with MSCV-neo retrovirus encoding empty vector (open triangles), wild-type Hoxa9 (filled triangles), or Hoxa9 Δ1-138 (A9del38; filled squares). Three different lines of Vp16-Meis1 progenitors were used for infection, and 400,000 G418-selected progenitors were plated in SCF-containing medium at day zero. Error bars represent standard deviations. (C) Southern blot analysis of Vp16-Meis1-retrovirus integration sites demonstrated the clonality of Vp16-Meis1 progenitors before (lane 1) and after expression of Hoxa9 (lane 2) or Hoxa7 (lane 3). Lane C, control progenitor line containing a different retroviral integration site. (D) Overall expression pattern of the 25 *Meis1*-related signature gene listed in Table 3, quantified using Affymetrix gene arrays in progenitors immortalized by Hoxa9 alone or with coexpressed Meis1 or by Vp16-Meis1 alone or superinfected with Hoxa9/a7 retrovirus. The *y* axis indicates relative mRNA intensity. (E) Comparison of expression levels of five representative *Meis1*-related signature genes shown in panel D and Table 3 among different progenitors, using real-time PCR. The template was first-strand cDNA produced by reverse transcription using pooled mRNA purified from two progenitor lines. Error bars represent the standard deviations from two repeated experiments.

TABLE 3. Gene expression profiling analysis of progenitors expressing Vp16-Meis1 or coexpressing Hox

Activation group and gene[b]	Gene description	GenBank accession no.	Transcript level score[a]				
			a9 (n = 5)	M+a9 (n = 5)	VM (n = 3)	VM+a9 (n = 3)	VM+a7 (n = 3)
Weak to moderate activation by Vp16-Meis1, further activation by Hox							
Cd34	Cd34 antigen	NM_133654	137	3,270	610	4,890	5,040
Flt3	Fms-like tyrosine kinase 3	NM_010229	<50	4,142	995	5,940	1,992
Il7r	Interleukin-7 receptor	NM_008372	<50	692	680	1,000	3,350
Crlr	Calcitonin receptor-like receptor	AF209905	<50	690	193	1,305	1,785
Msi2h	Musashi homologue 2; RNA-binding protein	BB418489	<50	756	145	3,875	1,425
Erg	v-Est-related gene	XM_622815	<50	884	70	625	1,775
Sox4	SRY box containing gene 4	NM_009238	536	1,376	1,050	2,795	1,310
Gpr56	G-protein-coupled receptor 56	AK141886	<40	126	50	575	990
Tilz1b	TSC22-related inducible leucine zipper 1b	AF201285	370	1,964	1,250	6,375	5,905
Ptprcap	CD45-associated protein	NM_016933	<50	1,160	520	1,400	2,035
Satb1	Special AT-rich sequence-binding protein	NM_009122	154	1,512	582	1,525	1,010
Ly86	MD1; lymphoid toll receptor	NM_010745	<50	1,350	513	1,900	2,300
Ngn/RC3	Neurogranin, protein kinase C substrate	AK002933	276	2,896	1,658	9,715	6,185
C1qR1	Complement subcomponent 1q, receptor 1	AK150385	630	3,030	1,308	4,900	2,875
Tmsb10	Thymosin beta-10	BB096368	1,080	6,320	1,718	6,350	3,175
Dbx4	DEAD (Asp-Glu-Ala-Asp) box 4	AK014844	<50	1,968	50	4,450	115
Ednra	Endothelin receptor type A	AK135555	<50	588	50	2,370	1,195
P2rx3	Purinergic receptor P2X, 3; ion channel	BC023089	<50	496	50	2,150	1,000
Kcna3	Potassium voltage-gated channel 3	AI323624	84	660	210	590	400
Wbscr15	Transmembrane adaptor protein	AF257136	170	1,374	258	1,075	1,500
Unknown	Unknown	AV365503	<50	402	395	4,875	920
Unknown	Unknown	BG071655	<50	418	113	550	405
Activation by Vp16-Meis1, no superactivation by Hox							
Nrip1	RIP140; Nuclear receptor-interacting protein	BB764550	60	310	255	283	500
Bcl2	B-cell leukemia/lymphoma 2; antiapoptosis	BI664467	514	2,660	1,415	1,400	1,925
Sesn3	Sestin 3	AK017464	70	836	605	825	370
Activation by Hox only							
c-*kit*	Stem cell factor receptor	X65997	2,350	2,390	831	3,850	2,675
Control							
Gapdh	Glyceraldehyde-3-phosphate dehydrogenase	BC083080	12,890	14,016	11,021	13,123	14,125
Actb	β-Actin	AK147787	13,530	15,168	13,200	14,125	16,450

[a] Score generated by the microarray scan program. M, Meis1; VM, Vp16-Meis1; a9, Hoxa9; a7, Hoxa7. The value of n represents the number of different immortalized progenitor lines (all cultured in SCF) that were used for analysis.
[b] Genes shown in bold have been implicated in the literature as either HSC markers or enriched in stem cell populations.

identified genes (*Msi2h*, *Sox4*, *Dbx4*, and *P2rx3*, plus two unknown genes) were activated by Hoxa9 in Vp16-Meis1 progenitors and expressed at much higher levels in Hoxa9-plus-Meis1 progenitors than in Hoxa9 progenitors, and they have been added to our list of *Meis1* signature genes (Table 3).

Vp16-Meis1 progenitors expressing *Hoxa9* or *Hoxa7* contained the same Vp16-Meis1 retroviral integration site as parental progenitors (Fig. 5C), ruling out the possibility that these dramatic transcriptional changes arose from selective expansion of an unrelated $Cd34^+$ $Flt3^+$ stem cell subpopulation that might still exist in cultures. Expression of Hoxa9 in Vp16-Meis1 progenitors reduced AML latency to an average of 24 days (Fig. 4A) and generated AML that was more similar to the myeloblastic phenotype (Fig. 4B, bottom panels), comprised of Lin^- and $MacI^+$ $B220^-$ subpopulations with high levels of Flt3 and Cd34 (Fig. 4F, bottom panels). This suggests that Hoxa9 and Hoxa7 participate in gene coactivation with Meis1.

The Hoxa9 N-terminal domain, which is essential for all transforming functions of Hoxa9, is dispensable for activating Flt3 expression and transforming properties in Vp16-Meis1-expressing progenitors, suggesting that it performs an activation function replaced by Vp16 on promoters co-occupied by Vp16-Meis1 and Hoxa9. The fact that fusion of Vp16 to Meis1 replaces Hox function, combined with the fact that both Meis1/Vp16-Meis1 and Hoxa9/a7 activate transcription of the same *Meis1*-related signature genes, favors a model in which Meis1, Hox, and Pbx directly bind these signature gene promoters that mediate leukemogenesis. If this model were correct, then Hoxa9 transactivation domains that are essential for activation of the *Meis1* signature genes in the context of wild-type Meis1 might be dispensable in the context of Vp16-Meis1. Indeed,

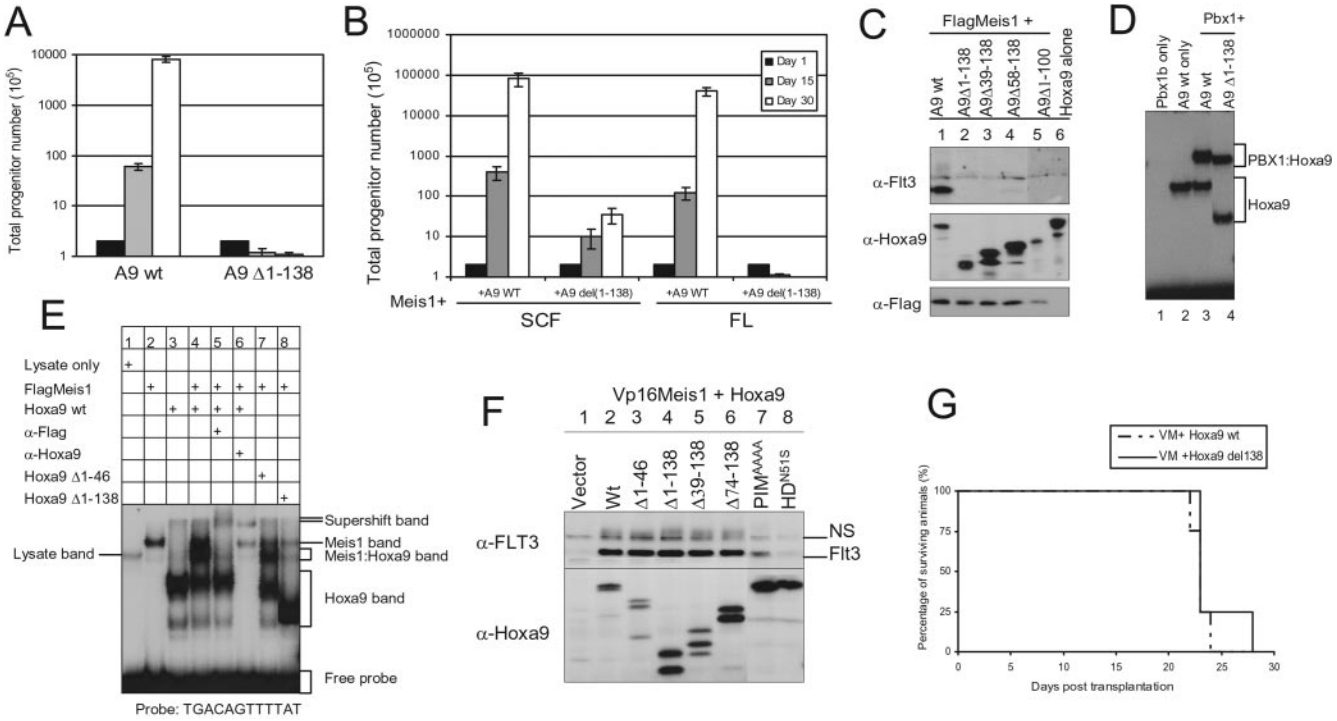

FIG. 6. The N-terminal residues 1 to 138 of Hoxa9 are dispensable for activation of *Flt3* and transformation in Vp16-Meis1-expressing progenitors but are required for Hoxa9-mediated immortalization and Meis1-cooperating functions in terms of *Flt3* activation and transformation. (A) Growth kinetics of primary bone marrow progenitors infected with retrovirus encoding either wild-type (WT) Hoxa9 or Hoxa9Δ1-138, followed by selection for 3 days in G418. The number of progenitors cultured in GM-CSF was counted on days 1 (solid bars), 15 (gray bars), and 30 (open bars) after drug selection. Error bars represent standard deviations of three duplicates. (B) Growth kinetics of primary ScaI$^+$ Lin$^-$-enriched progenitors infected with a 1:1 mixture of retrovirus encoding Meis1 and that encoding Hoxa9 (WT or Δ138), followed by dual drug resistance selection and cultivation in SCF or FL. Duplicate cultures were evaluated, and error bars indicate standard deviations. (C) Expression of Flt3, Hoxa9, and Flag-Meis1, 2 weeks after coinfection (as for panel B, with SCF and dual selection) of ScaI$^+$ Lin$^-$-enriched marrow progenitors with retrovirus encoding Flag-Meis1 and Hoxa9. (D) Heterodimer formation between Pbx1 and Hoxa9 examined by EMSA on the DNA element TGATTTAT. The identity of proteins added to the binding reaction mixture is indicated above each lane. (E) Interaction between Meis1a and wild-type or mutant Hoxa9 examined by EMSA to the DNA probe TGACAGTTTTAT. Recombinant proteins produced by coupled transcription-translation were lysate only (lane 1), Flag-Meis1 (lane 2), Hoxa9 (lane 3), and Flag-Meis1 plus Hoxa9 (lanes 4 to 8). Antibody against Flag-Meis1 (lane 5) or Hoxa9 (lane 6) was added to supershift protein-DNA complexes. (F) Expression levels of Flt3 and Hoxa9 in Vp16-Meis1 progenitors 3 weeks after retroviral expression of wild-type or mutant forms of Hoxa9 followed by drug selection in SCF-containing medium. (G) Survival curves of mice intravenously injected with 1×10^6 Vp16-Meis1 progenitors superinfected with retrovirus encoding Hoxa9 WT ($n = 4$) or Δ138 ($n = 4$).

the Hoxa9 NTD (residues 1 to 138), which has been reported to contain a transactivation domain and Meis1 interaction motif (41), which is essential for immortalization by Hoxa9 alone in GM-CSF (Fig. 6A) or in SCF (not shown), is essential for immortalization of SCF- or FL-dependent progenitors with Meis1 (Fig. 6B), and is essential for Meis1-dependent production of Flt3 in infected ScaI$^+$ Lin$^-$ marrow progenitors (Fig. 6C, lanes 2 to 5 versus lane 1), was dispensable for Hoxa9-induced proliferation (Fig. 5B), for Flt3 up-regulation (Fig. 6F, lane 4 versus lane 2) in Vp16-Meis1 progenitors, or for increasing the aggressiveness of leukemias produced by Vp16-Meis1 progenitors (Fig. 6G). By contrast, the DNA binding and Pbx interaction mutants Hoxa9-HD^{N51S} and Hoxa9-PIM^{AAAA} (7) exhibited no activation or minimal activation (25% of wild type) of *Flt3* transcription (Fig. 6F, lanes 7 and 8 versus lane 2). Hoxa9Δ1-138 retained its ability to interact with Pbx1 on DNA (Fig. 6D, lane 3 versus lane 4) and lost its heterodimerization abilities with Meis1 on DNA (Fig. 6E, lane 4 versus lane 8). The fact that the NTD of Hoxa9 is dispensable for Hoxa9 transforming functions in Vp16-Meis1 progenitors suggests that its transactivation function is replaced by the persistent transactivation function of a Vp16-Meis1 complex bound to an adjacent DNA element.

Hoxa9 and Meis1 directly bind the *Flt3* proximal promoter and 5′ enhancer regions. ChIP was used to examine whether Hoxa9 and Meis1 bind the promoter of *Flt3*, the prototypic *Meis1* signature gene whose transcription is further augmented by either Hoxa9 or Hoxa7. Primers were designed to randomly cover 10-kb upstream *Flt3* promoter/enhancer sequences (Fig. 7A). ChIP demonstrated that Hoxa9 was recruited to the proximal promoter (P3) and 5′ enhancer regions (P5 and P6) in progenitors expressing either *Hoxa9* alone or coexpressing *Meis1* plus *Hoxa9* (Fig. 7B) and that Meis1 (Flag tagged; anti-Flag used for ChIP) was recruited to loci P3, P5, and P6 only in progenitors immortalized by *Hoxa9* plus *Meis1*. The same ChIP results were observed using antibodies against the N terminus or homeodomain of Meis1 (data not shown). Interestingly, recruitment of Meis1 was accompanied by acet-

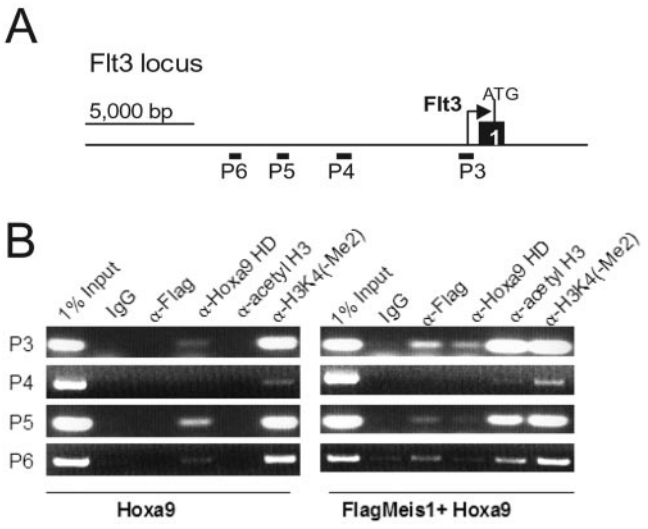

FIG. 7. Meis1 and Hoxa9 bind to the *Flt3* proximal and distal promoter regions. (A) Schematic of the murine *Flt3* locus. Black boxes represent exons, and the arrowhead represents the putative transcription start site. Black bars P3 to -6 designate positions of the amplicons used in ChIP analysis; ATG indicates the position of the initiation methionine. (B) ChIP analysis examining the recruitment of Hoxa9 and Flag-Meis1 and the status of histone modification on *Flt3* promoters (loci P3 to P6) in myeloid progenitors immortalized by Hoxa9 alone or by both Hoxa9 and Flag-Meis1. Lanes were loaded with products of PCR amplification using template prepared from either 1% sheared chromatin (input control) or immunoprecipitated chromatin using nonspecific antibodies (IgG) or specific antibodies against the Flag tag, the homoedomain of Hoxa9, acetylated histone H3, or dimethylated histone 3 Lys 4 (H3K4).

ylation of histone H3 along *Flt3* promoter and enhancer regions, while both cell lines exhibited dimethylation of histone H3 Lys 4 (H3K4) within the same regions. All signals were specific, based on the cell type specificity and precipitation control results using nonspecific IgG. These results indicate that Meis1 may induce histone acetylation prior to activation of *Flt3* transcription.

DISCUSSION

Here we demonstrated that in the absence of coexpressed *Hox* genes, a dominant activating form of Meis1 (Vp16-Meis1) sustains self-renewal of undifferentiated hematopoietic progenitors that exhibit leukemic potential in vivo, functions that are not possessed by either wild-type Meis1 or the dominant repressive form of Meis1, en-Meis1. We then demonstrated that Vp16-Meis1 mimics the combined functions of Hoxa9 and Meis1 in terms of activating expression of *Meis1*-related signature genes, albeit at low levels, which are characteristically expressed in leukemic progenitors immortalized by Hoxa9 plus Meis1 but not in nonleukemic progenitors immortalized by Hoxa9 alone. Next, we demonstrated that Hoxa9 and Hoxa7 further augment transcription of most of these *Meis1* signature genes (*Hox*/*Meis1* signature genes, as a more proper definition), indicating that their transcription is driven by the combined functions of Meis1 and Hoxa7/a9 functions in AML. The mechanism of cooperativity is implicated as promoter co-occupancy by Hoxa7/a9 and Pbx1/2-Meis1 complexes, based on the result that fusion of the Vp16 domain to Meis1 replaced both the essential function of the Hoxa9 NTD and the Meis1 CTD and was verified as such for the *Flt3* promoter, using ChIP analysis. Collectively, our data support a model in which a subset of leukemogenesis-related promoters are directly bound and activated by complexes containing Hoxa7/a9, Meis1, and Pbx1/2.

Four transcriptional principles related to Meis1 and its interacting cofactors in hematopoietic progenitors are suggested by our analysis. First, the fact that Vp16-Meis1–Pbx complexes enforce self-renewal of leukemic stem cells in vivo suggests that Meis1-Pbx complexes regulate progenitor expansion during normal hematopoiesis by activating target gene transcription. Second, the fact that Hoxa7 and Hoxa9 augment expression of *Meis1* signature genes in Vp16-Meis1 progenitors suggests that Hox proteins actively participate in transactivation of *Meis1*-related signature genes in normal hematopoiesis. Prior to this report, there was no evidence that Hoxa7 or Hoxa9 controlled expression of Meis1 target genes in leukemia. Third, the mutational analysis of Hoxa9 and Meis1 domains critical for their functions in Vp16-Meis1 progenitors suggests a model in which all three homeodomain proteins—Pbx1/2, Meis1, and Hoxa7/a9—cooperate on single promoters critical for establishing the leukemogenic stem cell phenotype (Fig. 8). Specifically, the Meis1 CTD and the Hoxa9 NTD may recruit cofactors harboring HAT activity (Fig. 8), functions replaced by the Vp16 domain in Vp16-Meis1. Fourth, the ability of the C-terminal half of Hoxa9 to activate transcription of *Flt3* in Vp16-Meis1 progenitors in a manner as robust as that

FIG. 8. Model of Pbx, Meis (Vp16-Meis1), and Hox complexes binding to a subset of promoters required for expression of leukemogenesis. Numbers near the arrowheads indicate the following transcriptional activities: 1, a signal-induced transactivation mediated by the Meis1 CTD; 2, Hoxa9-NTD-mediated transactivation; 3, transactivation function mediated by the Hoxa9 C-terminal half, residues 139 to 271; 4, transactivation by the Vp16 domain fused onto Meis1, by recruiting HAT. The Vp16 domain replaces the function mediated by the Meis1 CTD and Hoxa9 NTD, suggesting that the Meis1 CTD and Hoxa9 CTD might recruit cofactors containing HAT activity and the Hoxa9 C-terminal half might utilize a different transactivation mechanism, such as recruiting factors harboring chromatin remodeling factor. AD, activation domain; RD, repression domain.

of wild-type *Hoxa9* suggests that this region possesses an additional transcriptional function which might be, for example, recruiting histone methyltransferase or chromatin remodeling factors (Fig. 8) that complements those provided by the Meis1 CTD and Hoxa9 NTD. The biochemical activities responsible for the N-terminal and C-terminal transactivating functions of Hoxa9 remain to be determined. This hypothesis, which is based on the genetic and cellular properties of leukemic progenitors, is consistent with physical interaction studies, which also found Meis1, Hoxa9, and Pbx2 in single nuclear complexes in myeloid cells (44), and reporter studies, which delineated cooperating functions of Meis1, Pbx1, and Hoxa1 proteins on regulation of the *Hoxb1/b2* enhancer (16, 21).

We also demonstrated that Hoxa7 is functionally redundant with Hoxa9 in terms of its Meis1-independent ability to arrest differentiation of nonleukemic progenitors and its Meis1-dependent function of targeting SCF- or FL-dependent leukemia-initiating progenitors that express *Flt3*. *Hoxa7* was originally identified as a locus coactivated with *Meis1* in BHX2 mouse leukemia (32) and activated in leukemia induced by large-scale retroviral insertional mutagenesis (23). *Hoxa7* was also suggested to be a crucial downstream mediator of MLL fusion oncoproteins (3, 50). Our results imply that Hoxa7, like Hoxa9, controls HSC expansion in cooperation with Meis1 and is likely to form interacting complexes. While Hoxa7 does not bind Meis1 in gel shift analysis (43), our data (as suggested by Hoxa9Δ1-138) suggest that it interacts with Pbx-Meis1 complexes via Pbx on target promoters as others have hypothesized previously (21). The promoter co-occupancy model would also account for leukemic cooperativity between Meis1 and Hoxb6/b3, which are also not predicted to bind Meis1 directly. We predict that coexpression of *Meis1* and *Hoxb6/b3* in SCF-dependent immortalized progenitors would also result in transcriptional activation of *Flt3* and other *Meis1* signature genes.

The *Hox/Meis1*-related signature genes that are coactivated by Meis1 plus Hox are involved in normal HSC biology and implicated in leukemogenesis. *Cd34* and *Flt3* are prominent HSC markers (1). Flt3 catalytic function is activated by mutations in over one-third of human AML, and we propose that *Flt3* expression permits expansion of LSCs in response to FL in stem cell niches. *Gpr56* (20), *Msi2h* (34), *Erg* (48), *C1qR1* (10, 48), and *Wbscr5* (48) are enriched in HSC or other tissue-type stem cells. The *Msi2h*-related gene *Msi1* is crucial for maintenance of neuronal stem cells (39). The *Ets*-related transcription factor *Erg* is fused to TLS/FUS and EWS in leukemia and Ewing sarcoma, respectively (14, 35). *Il7r* is important for lymphoid progenitor expansion, and *Gpr56* is overexpressed in brain tumors and mutated in a genetic disorder involving brain cortical malformation (36, 42). It is possible that up-regulation of the *Grb2*-interacting adaptor *Wbscr5/LAB* (22) contributes to specific signaling pathways in HSCs. Understanding functions of these genes will cast additional light on how they contribute to the LSC phenotype.

Previous studies reported over 200 genes regulated by Hoxa9 in leukemia cell lines or in $CD34^+$ HSCs (11, 12), but with the exception of *Erg*, these genes do not include the *Hox/Meis1*-activated signature genes examined herein. It is possible that studies using leukemia cell lines do not identify these signature genes because such genes are already expressed at high basal levels in the control parental progenitors. Alternatively, these *Hox/Meis1* signature genes may not be activated by introduction of exogenous *Hoxa9* if progenitors do not express essential cofactors, such as *Meis1*. Indeed, Hoxa9 alone does not activate any of the signature genes, as exhibited by Hoxa9-immortalized progenitors. When exogenous Hoxa9 is expressed in normal $CD34^+$ HSCs, the expression of endogenous *Hox* and *Meis1* may preclude significant further activation of these *Hox/Meis1* signature genes. The heterogeneity of this population may also dilute the strong response of responsive subsets that express required cofactors. By contrast, because Vp16Meis1 progenitors lack *Hox* gene expression, they may be particularly sensitive to transcriptional regulatory mechanisms induced by *Hox* and, because they are uniform populations, the impact of *Hox* genes is maximized. Thus, Vp16-Meis1 progenitors may represent a unique tool for determining both the specificity and biochemical mechanisms of *Hoxa7* and *Hoxa9* gene activation in AML.

ACKNOWLEDGMENTS

This work is supported by Public Health Service grant NIH CA56876 awarded to M.P.K.

We thank Dennis Young for assistance with FACS analysis and Joe Aguilera for assistance with mouse radiation (UCSD Cancer Center Shared Resources). We give special thanks to Mark Featherstone, Corey Largman, Robert Slany, and Adi Salzberg for providing reagents for work related to this paper.

REFERENCES

1. **Adolfsson, J., R. Mansson, N. Buza-Vidas, A. Hultquist, K. Liuba, C. T. Jensen, D. Bryder, L. Yang, O. J. Borge, L. A. Thoren, K. Anderson, E. Sitnicka, Y. Sasaki, M. Sigvardsson, and S. E. Jacobsen.** 2005. Identification of $Flt3^+$ lympho-myeloid stem cells lacking erythro-megakaryocytic potential a revised road map for adult blood lineage commitment. Cell **121:**295–306.
2. **Afonja, O., J. E. Smith, Jr., D. M. Cheng, A. S. Goldenberg, E. Amorosi, T. Shimamoto, S. Nakamura, K. Ohyashiki, J. Ohyashiki, K. Toyama, and K. Takeshita.** 2000. MEIS1 and HOXA7 genes in human acute myeloid leukemia. Leuk. Res. **24:**849–855.
3. **Ayton, P. M., and M. L. Cleary.** 2003. Transformation of myeloid progenitors by MLL oncoproteins is dependent on Hoxa7 and Hoxa9. Genes Dev. **17:**2298–2307.
4. **Azcoitia, V., M. Aracil, A. C. Martinez, and M. Torres.** 2005. The homeodomain protein Meis1 is essential for definitive hematopoiesis and vascular patterning in the mouse embryo. Dev. Biol. **280:**307–320.
5. **Bei, L., Y. Lu, and E. A. Eklund.** 2005. HOXA9 activates transcription of the gene encoding gp91Phox during myeloid differentiation. J. Biol. Chem. **280:** 12359–12370.
6. **Berkes, C. A., D. A. Bergstrom, B. H. Penn, K. J. Seaver, P. S. Knoepfler, and S. J. Tapscott.** 2004. Pbx marks genes for activation by MyoD indicating a role for a homeodomain protein in establishing myogenic potential. Mol. Cell **14:**465–477.
7. **Calvo, K. R., D. B. Sykes, M. Pasillas, and M. P. Kamps.** 2000. Hoxa9 immortalizes a granulocyte-macrophage colony-stimulating factor-dependent promyelocyte capable of biphenotypic differentiation to neutrophils or macrophages, independent of enforced Meis expression. Mol. Cell. Biol. **20:**3274–3285.
8. **Calvo, K. R., D. B. Sykes, M. P. Pasillas, and M. P. Kamps.** 2002. Nup98-HoxA9 immortalizes myeloid progenitors, enforces expression of Hoxa9, Hoxa7, and Meis1, and alters cytokine-specific responses in a manner similar to that induced by retroviral co-expression of Hoxa9 and Meis1. Oncogene **21:**4247–4256.
9. **Chang, C. P., Y. Jacobs, T. Nakamura, N. A. Jenkins, N. G. Copeland, and M. L. Cleary.** 1997. Meis proteins are major in vivo DNA binding partners for wild-type but not chimeric Pbx proteins. Mol. Cell. Biol. **17:**5679–5687.
10. **Danet, G. H., J. L. Luongo, G. Butler, M. M. Lu, A. J. Tenner, M. C. Simon, and D. A. Bonnet.** 2002. C1qRp defines a new human stem cell population with hematopoietic and hepatic potential. Proc. Natl. Acad. Sci. USA **99:** 10441–10445.
11. **Dorsam, S. T., C. M. Ferrell, G. P. Dorsam, M. K. Derynck, U. Vijapurkar, D. Khodabakhsh, B. Pau, H. Bernstein, C. M. Haqq, C. Largman, and H. J. Lawrence.** 2004. The transcriptome of the leukemogenic homeoprotein HOXA9 in human hematopoietic cells. Blood **103:**1676–1684.
12. **Ferrell, C. M., S. T. Dorsam, H. Ohta, R. K. Humphries, M. K. Derynck, C. Haqq, C. Largman, and H. J. Lawrence.** 2005. Activation of stem-cell specific

genes by HOXA9 and HOXA10 homeodomain proteins in CD34$^+$ human cord blood cells. Stem Cells **23:**644–655.

13. **Fischbach, N. A., S. Rozenfeld, W. Shen, S. Fong, D. Chrobak, D. Ginzinger, S. C. Kogan, A. Radhakrishnan, M. M. Le Beau, C. Largman, and H. J. Lawrence.** 2005. HOXB6 overexpression in murine bone marrow immortalizes a myelomonocytic precursor in vitro and causes hematopoietic stem cell expansion and acute myeloid leukemia in vivo. Blood **105:**1456–1466.
14. **Giovannini, M., J. A. Biegel, M. Serra, J. Y. Wang, Y. H. Wei, L. Nycum, B. S. Emanuel, and G. A. Evans.** 1994. EWS-erg and EWS-Fli1 fusion transcripts in Ewing's sarcoma and primitive neuroectodermal tumors with variant translocations. J. Clin. Investig. **94:**489–496.
15. **Hisa, T., S. E. Spence, R. A. Rachel, M. Fujita, T. Nakamura, J. M. Ward, D. E. Devor-Henneman, Y. Saiki, H. Kutsuna, L. Tessarollo, N. A. Jenkins, and N. G. Copeland.** 2004. Hematopoietic, angiogenic and eye defects in Meis1 mutant animals. EMBO J. **23:**450–459.
16. **Huang, H., M. Rastegar, C. Bodner, S. L. Goh, I. Rambaldi, and M. Featherstone.** 2005. MEIS C termini harbor transcriptional activation domains that respond to cell signaling. J. Biol. Chem. **280:**10119–10127.
17. **Imamura, T., A. Morimoto, M. Takanashi, S. Hibi, T. Sugimoto, E. Ishii, and S. Imashuku.** 2002. Frequent co-expression of HoxA9 and Meis1 genes in infant acute lymphoblastic leukaemia with MLL rearrangement. Br. J. Haematol. **119:**119–121.
18. **Inbal, A., N. Halachmi, C. Dibner, D. Frank, and A. Salzberg.** 2001. Genetic evidence for the transcriptional-activating function of Homothorax during adult fly development. Development **128:**3405–3413.
19. **Irizarry, R. A., B. Hobbs, F. Collin, Y. D. Beazer-Barclay, K. J. Antonellis, U. Scherf, and T. P. Speed.** 2003. Exploration, normalization, and summaries of high density oligonucleotide array probe level data. Biostatistics **4:**249–264.
20. **Ivanova, N. B., J. T. Dimos, C. Schaniel, J. A. Hackney, K. A. Moore, and I. R. Lemischka.** 2002. A stem cell molecular signature. Science **298:**601–604.
21. **Jacobs, Y., C. A. Schnabel, and M. L. Cleary.** 1999. Trimeric association of Hox and TALE homeodomain proteins mediates Hoxb2 hindbrain enhancer activity. Mol. Cell. Biol. **19:**5134–5142.
22. **Janssen, E., M. Zhu, W. Zhang, and S. Koonpaew.** 2003. LAB: a new membrane-associated adaptor molecule in B cell activation. Nat. Immunol. **4:**117–123.
23. **Joosten, M., Y. Vankan-Berkhoudt, M. Tas, M. Lunghi, Y. Jenniskens, E. Parganas, P. J. Valk, B. Lowenberg, E. van den Akker, and R. Delwel.** 2002. Large-scale identification of novel potential disease loci in mouse leukemia applying an improved strategy for cloning common virus integration sites. Oncogene **21:**7247–7255.
24. **Kamps, M. P., C. Murre, X. H. Sun, and D. Baltimore.** 1990. A new homeobox gene contributes the DNA binding domain of the t(1;19) translocation protein in pre-B ALL. Cell **60:**547–555.
25. **Kamps, M. P., D. D. Wright, and Q. Lu.** 1996. DNA-binding by oncoprotein E2a-Pbx1 is important for blocking differentiation but dispensable for fibroblast transformation. Oncogene **12:**19–30.
26. **Knoepfler, P. S., K. R. Calvo, H. Chen, S. E. Antonarakis, and M. P. Kamps.** 1997. Meis1 and pKnox1 bind DNA cooperatively with Pbx1 utilizing an interaction surface disrupted in oncoprotein E2a-Pbx1. Proc. Natl. Acad. Sci. USA **94:**14553–14558.
27. **Knoepfler, P. S., and M. P. Kamps.** 1997. The highest affinity DNA element bound by Pbx complexes in t(1;19) leukemic cells fails to mediate cooperative DNA-binding or cooperative transactivation by E2a-Pbx1 and class I Hox proteins: evidence for selective targetting of E2a-Pbx1 to a subset of Pbx-recognition elements. Oncogene **14:**2521–2531.
28. **Kroon, E., J. Krosl, U. Thorsteinsdottir, S. Baban, A. M. Buchberg, and G. Sauvageau.** 1998. Hoxa9 transforms primary bone marrow cells through specific collaboration with Meis1a but not Pbx1b. EMBO J. **17:**3714–3725.
29. **Lawrence, H. J., J. Christensen, S. Fong, Y. L. Hu, I. Weissman, G. Sauvageau, R. K. Humphries, and C. Largman.** 2005. Loss of expression of the HOXA-9 homeobox gene impairs the proliferation and repopulating ability of hematopoietic stem cells. Blood **106:**3988–3994.
30. **Lawrence, H. J., S. Rozenfeld, C. Cruz, K. Matsukuma, A. Kwong, L. Komuves, A. M. Buchberg, and C. Largman.** 1999. Frequent co-expression of the HOXA9 and MEIS1 homeobox genes in human myeloid leukemias. Leukemia **13:**1993–1999.
31. **Memedula, S., and A. S. Belmont.** 2003. Sequential recruitment of HAT and SWI/SNF components to condensed chromatin by VP16. Curr. Biol. **13:**241–246.
32. **Moskow, J. J., F. Bullrich, K. Huebner, I. O. Daar, and A. M. Buchberg.** 1995. Meis1, a PBX1-related homeobox gene involved in myeloid leukemia in BXH-2 mice. Mol. Cell. Biol. **15:**5434–5443.
33. **Nakamura, T., D. A. Largaespada, J. D. Shaughnessy, Jr., N. A. Jenkins, and N. G. Copeland.** 1996. Cooperative activation of Hoxa and Pbx1-related genes in murine myeloid leukaemias. Nat. Genet. **12:**149–153.
34. **Okano, H., T. Imai, and M. Okabe.** 2002. Musashi: a translational regulator of cell fate. J. Cell Sci. **115:**1355–1359.
35. **Pereira, D. S., C. Dorrell, C. Y. Ito, O. I. Gan, B. Murdoch, V. N. Rao, J. P. Zou, E. S. Reddy, and J. E. Dick.** 1998. Retroviral transduction of TLS-ERG initiates a leukemogenic program in normal human hematopoietic cells. Proc. Natl. Acad. Sci. USA **95:**8239–8244.
36. **Piao, X., R. S. Hill, A. Bodell, B. S. Chang, L. Basel-Vanagaite, R. Straussberg, W. B. Dobyns, B. Qasrawi, R. M. Winter, A. M. Innes, T. Voit, M. E. Ross, J. L. Michaud, J. C. Descarie, A. J. Barkovich, and C. A. Walsh.** 2004. G protein-coupled receptor-dependent development of human frontal cortex. Science **303:**2033–2036.
37. **Pineault, N., C. D. Helgason, H. J. Lawrence, and R. K. Humphries.** 2002. Differential expression of Hox, Meis1, and Pbx1 genes in primitive cells throughout murine hematopoietic ontogeny. Exp. Hematol. **30:**49–57.
38. **Rave-Harel, N., M. L. Givens, S. B. Nelson, H. A. Duong, D. Coss, M. E. Clark, S. B. Hall, M. P. Kamps, and P. L. Mellon.** 2004. TALE homeodomain proteins regulate gonadotropin-releasing hormone gene expression independently and via interactions with Oct-1. J. Biol. Chem. **279:**30287–30297.
39. **Sakakibara, S., Y. Nakamura, T. Yoshida, S. Shibata, M. Koike, H. Takano, S. Ueda, Y. Uchiyama, T. Noda, and H. Okano.** 2002. RNA-binding protein Musashi family: roles for CNS stem cells and a subpopulation of ependymal cells revealed by targeted disruption and antisense ablation. Proc. Natl. Acad. Sci. USA **99:**15194–15199.
40. **Saleh, M., I. Rambaldi, X. J. Yang, and M. S. Featherstone.** 2000. Cell signaling switches HOX-PBX complexes from repressors to activators of transcription mediated by histone deacetylases and histone acetyltransferases. Mol. Cell. Biol. **20:**8623–8633.
41. **Schnabel, C. A., Y. Jacobs, and M. L. Cleary.** 2000. HoxA9-mediated immortalization of myeloid progenitors requires functional interactions with TALE cofactors Pbx and Meis. Oncogene **19:**608–616.
42. **Shashidhar, S., G. Lorente, U. Nagavarapu, A. Nelson, J. Kuo, J. Cummins, K. Nikolich, R. Urfer, and E. D. Foehr.** 2005. GPR56 is a GPCR that is overexpressed in gliomas and functions in tumor cell adhesion. Oncogene **24:**1673–1682.
43. **Shen, W. F., J. C. Montgomery, S. Rozenfeld, J. J. Moskow, H. J. Lawrence, A. M. Buchberg, and C. Largman.** 1997. AbdB-like Hox proteins stabilize DNA binding by the Meis1 homeodomain proteins. Mol. Cell. Biol. **17:**6448–6458.
44. **Shen, W. F., S. Rozenfeld, A. Kwong, L. G. Kömüves, H. J. Lawrence, and C. Largman.** 1999. HOXA9 forms triple complexes with PBX2 and MEIS1 in myeloid cells. Mol. Cell. Biol. **19:**3051–3061.
45. **Sykes, D. B., and M. P. Kamps.** 2004. E2a/Pbx1 induces the rapid proliferation of stem cell factor-dependent murine pro-T cells that cause acute T-lymphoid or myeloid leukemias in mice. Mol. Cell. Biol. **24:**1256–1269.
46. **Thorsteinsdottir, U., E. Kroon, L. Jerome, F. Blasi, and G. Sauvageau.** 2001. Defining roles for HOX and MEIS1 genes in induction of acute myeloid leukemia. Mol. Cell. Biol. **21:**224–234.
47. **Thorsteinsdottir, U., A. Mamo, E. Kroon, L. Jerome, J. Bijl, H. J. Lawrence, K. Humphries, and G. Sauvageau.** 2002. Overexpression of the myeloid leukemia-associated Hoxa9 gene in bone marrow cells induces stem cell expansion. Blood **99:**121–129.
48. **Wagner, W., A. Ansorge, U. Wirkner, V. Eckstein, C. Schwager, J. Blake, K. Miesala, J. Selig, R. Saffrich, W. Ansorge, and A. D. Ho.** 2004. Molecular evidence for stem cell function of the slow-dividing fraction among human hematopoietic progenitor cells by genome-wide analysis. Blood **104:**675–686.
49. **Wang, G. G., M. P. Pasillas, and M. P. Kamps.** 2005. Meis1 programs transcription of FLT3 and cancer stem cell character, using a mechanism that requires interaction with Pbx and a novel function of the Meis1 C-terminus. Blood **106:**254–264.
50. **Zeisig, B. B., T. Milne, M. P. Garcia-Cuellar, S. Schreiner, M. E. Martin, U. Fuchs, A. Borkhardt, S. K. Chanda, J. Walker, R. Soden, J. L. Hess, and R. K. Slany.** 2004. Hoxa9 and Meis1 are key targets for MLL-ENL-mediated cellular immortalization. Mol. Cell. Biol. **24:**617–628.
51. **Zhang, X., A. Friedman, S. Heaney, P. Purcell, and R. L. Maas.** 2002. Meis homeoproteins directly regulate Pax6 during vertebrate lens morphogenesis. Genes Dev. **16:**2097–2107.